

Cite this: *J. Mater. Chem. B*,  
2024, 12, 10466

# Atomically dispersed single-atom catalysts (SACs) and enzymes (SAzymes): synthesis and application in Alzheimer's disease detection

Himanshi Goel,<sup>a</sup> Ishika Rana,<sup>a</sup> Kajal Jain,<sup>a</sup> Kumar Rakesh Ranjan\*<sup>a</sup> and Vivek Mishra \*<sup>b</sup>

Alzheimer's disease (AD) is a progressive neurodegenerative disorder characterized by cognitive decline and memory loss. Conventional diagnostic methods, such as neuroimaging and cerebrospinal fluid analysis, typically detect AD at advanced stages, limiting the efficacy of therapeutic interventions. Early detection is crucial for improving patient condition by enabling timely administration of treatments that may decelerate disease progression. In this context, single-atom catalysts (SACs) and single-atom nanozymes (SAzymes) have emerged as promising tools offering highly sensitive and selective detection of Alzheimer's biomarkers. SACs, consisting of isolated metal atoms on a support surface, deliver unparalleled atomic efficiency, increased reactivity, and reduced operational costs, although certain challenges in terms of stability, aggregation, and other factors persist. The advent of SAzymes, which integrate SACs with natural metalloprotease catalysts, has further advanced this field by enabling controlled electronic exchange, synergistic productivity, and enhanced biosafety. Particularly, M–N–C SACs with M–N<sub>x</sub> active sites mimic the selectivity and sensitivity of natural metalloenzymes, providing a robust platform for early detection of AD. This review encompasses the advancements in SACs and SAzymes, highlighting their pivotal role in bridging the gap between conventional enzymes and nanozyme and offering enhanced catalytic efficiency, controlled electron transfer, and improved biosafety for Alzheimer's detection.

Received 13th June 2024,  
Accepted 2nd September 2024

DOI: 10.1039/d4tb01293c

rsc.li/materials-b

## 1. Introduction

Catalysis is a fundamental process that accelerates chemical reactions by reducing activation energy, with the catalyst itself remaining unchanged. In this regard, heterogeneous catalysts have gained more interest.<sup>1–8</sup> In heterogeneous catalysis, the catalyst and reactants are in different phases with multiple active sites, often with solid catalysts facilitating reactions in liquid or gaseous environments. This phase separation is particularly advantageous in industrial applications as it simplifies the recovery and reuse of the catalyst.<sup>9</sup> Compared with conventional catalysts, where many atoms remain inactive within the bulk material, nanocatalysts<sup>8</sup> represent a significant advancement, operating at the nanoscale (particles with a size typically below 100 nm) and offering enhanced properties due to their large surface area and unique quantum effects. Further downsizing of nanocatalysts has emerged as a strategy to

enhance catalytic activity by increasing the surface area available for reactions. As catalysts are reduced to the nanoscale, their efficiency is significantly improved owing to the larger proportion of atoms exposed on the surface. This approach has culminated in the development of single-atom catalysts (SACs), where individual metal atoms are dispersed on a support material.<sup>10–12</sup>

Single-atom catalysts (SACs) mark a significant advancement in heterogeneous catalysis,<sup>13–18</sup> primarily due to their ability to achieve maximized atomic efficiency. Unlike conventional catalysts, SACs ensure that each metal atom is fully exposed and actively participates in the catalytic process. This increased atomic utilization not only enhances catalytic activity but also significantly reduces the number of precious metals required, making SACs both cost-effective and resource-efficient.<sup>10,19–21</sup> One of the defining features of SACs is their distinct electronic structure. The isolation of individual metal atoms creates unique electronic configurations, leading to enhanced reactivity and selectivity. This allows SACs to interact more effectively with biomolecules, facilitating more efficient catalytic processes. Moreover, the interaction between single metal atoms and the support material, such as graphene or metal oxides, is critical in shaping the catalytic behaviour of

<sup>a</sup> Amity Institute of Applied Sciences, Amity University Noida, UP, India.  
E-mail: krranjan@amity.edu

<sup>b</sup> Amity Institute of Click Chemistry Research and Studies, Amity University Noida, UP, India. E-mail: vmishra@amity.edu

SACs.<sup>22,23</sup> These metal–support interactions can generate new active sites that are absent in bulk catalysts, further boosting the catalytic performance. SACs also exhibit high thermal stability, a key attribute for their application in high-temperature industrial processes. The incorporation of heteroatoms, such as nitrogen, sulfur, or oxygen, into the support structure can significantly modulate the electronic environment around the single metal atoms, offering tuneable catalytic properties that can be tailored for the pathological conditions of biosystems.<sup>24,25</sup>

Building on the concept of SACs, single-atom catalysts have been adapted into SAzymes,<sup>26</sup> which were designed to mimic the high specificity and efficiency of natural enzymes.<sup>27</sup> SAzymes combine the reactivity of single atoms with the selectivity and substrate recognition capabilities of natural enzymes.<sup>28</sup> This combo (SAzymes) bridges the gap between natural enzymes and nanozymes and serves as a new frontier in the biomedical field.<sup>29,30</sup> SAzymes offer controlled electronic transfer, unique catalytic pathways, greater catalytic efficiency (10–100 times better than nanozymes), versatile catalytic selectivity, and biosafety for sophisticated practical applications in bacterial disinfectant applications, wound healing, biosensing, organic pollutants degradation, tumour therapy, Alzheimer's therapy, and many more.<sup>31–33</sup> Recently, M–N–C SACs (M = Fe, Au, Co, Ru, Rh, Pd, Ir, *etc.*) with M–N<sub>x</sub> active sites have gained more attention as their electronic, structural, and chemical properties are related more closely to natural metalloenzymes, such as oxyhaemoglobin, cytochrome-P<sub>450</sub> enzymes, and horseradish peroxidase. They are more selective and sensitive than nanozymes. They possess unique active sites for both homogenous and heterogenous catalysis, and their structure–activity relationships can be interpreted from DFT calculations.<sup>34,35</sup>

SACs and SAzymes have been widely used in various fields over the years of their development, as discussed in Table 1. One of the most compelling applications of SACs and SAzymes is in the detection and treatment of neurodegenerative diseases, such as Alzheimer's disease. Alzheimer's disease (AD), characterized by the accumulation of amyloid-beta plaques and neurofibrillary tangles, is a complex condition with a multifactorial aetiology.<sup>36,37</sup> Traditional diagnostic and therapeutic approaches have had limited success, necessitating the exploration of novel strategies. SACs and SAzymes offer the potential for highly sensitive detection methods. The enzyme-like behaviour of SAzymes, coupled with the precise control over their active sites, could significantly improve the early detection and management of Alzheimer's disease. This application highlights the potential of nanotechnology and catalysis to address critical challenges in medical diagnostics.<sup>38–41</sup>

Table 1 illustrates the details of some reported single-atom catalysts (SACs) and single-atom nanozymes (SANs), utilizing metals like Au, Pt, Fe, and Cu, which are advanced materials with diverse applications, including for Alzheimer's disease detection. These have been synthesized through methods like pyrolysis and solvothermal processes, resulting in diverse structures from core–shell configurations to atomically dispersed sites. These materials exhibit enzymatic activities, such as oxidase, peroxidase, and Fenton-like reactions, which are

crucial for enhancing biosensing and therapeutic applications. For Alzheimer's detection, SACs like FeNCP/NW and Fe–N<sub>x</sub> SANs have demonstrated high sensitivity, with detection limits of 0.96 μM and 0.88 pg mL<sup>-1</sup> for key biomarkers, respectively. Their advantages include high selectivity and cost effectiveness, although certain challenges, like a low metal loading and stability, persist. Despite these issues, SACs and SANs represent promising tools for improving early diagnosis and intervention in Alzheimer's disease.

## 2. Synthesis strategies of SACs

Synthesizing single-atom catalysts (SACs) with a high degree of atomic dispersion is challenging due to the great surface energy, which induces metal atom aggregation. The single atoms within these catalysts also tend to aggregate during catalytic processes. Consequently, establishing robust coordination environments is essential to stabilize these single-atom sites, ensuring elevated metal loading capacity, activity, and durability in catalytic applications. Some commonly used techniques for the synthesis of SACs reported so far include pyrolysis,<sup>68,69</sup> wet chemistry approaches,<sup>70–72</sup> atomic layer deposition,<sup>73,74</sup> and the mass-selected soft-landing method.<sup>75–77</sup> Among the various synthetic approaches for SACs, the focus has grown on the utilization of oxygen-deficient supports to anchor individual metal atoms, as an elevated density of active sites can be achieved with selectively controlled chemical reactions as well as stability.<sup>78,79</sup>

The current challenge with techniques such as co-precipitation, ion exchange, impregnation, and hydrothermal treatment is their scalability. However, when these techniques are scaled up, the consistent transfer of mass and heat becomes an issue, often leading to uneven localized concentrations. This unevenness tends to cause agglomeration, where noble metal components cluster together.<sup>80,81</sup> Another concern arises from selective leaching, such as when employing a NaCN solution to eliminate nanoparticles while keeping intact the isolated metal ions anchored to the support and in template assistance when initially using zeolites as templates and subsequently removing them with a concentrated acidic solution, which generates substantial volumes of liquid waste, thereby raising environmental toxicity. Also, producing SACs is generally expensive and has low production efficiency.<sup>82</sup>

## 3. Chemical stability of SACs

In recent years, there has been growing interest in the use of noble metals that are dispersed at the atomic level on solid oxide supports in the field of heterogeneous catalysis.<sup>83</sup> Achieving the highest possible atom efficiency is a primary objective, and the stability of SACs plays a crucial role in this pursuit. One significant challenge often encountered is the limited stability of these supported single atoms when exposed to operating conditions, primarily because the metal atoms in SACs tend to be undercoordinated. To create well-defined SACs, researchers typically employ a low metal loading on a substrate. Increasing the amount of metal loaded onto the substrate often leads to the

Table 1 Parameters of different SACs/SANs with unique active sites incorporated in various fields

SAC/Sazymes	Metal Active site	Metal loading (wt%)	Supporting precursor	Synthesis	Structure	Enzymatic activity	Catalytic mechanism	Applications	Advantages and practical implication	Limitations	Efficiency	Ref.
FeNCP/NW (SAC)	Fe	14.9%	P-Fe polypyrrole nanowires (P-Fe-PPy NWs)	One-pot hydro-thermal method ( $N_2/NH_3$ atmosphere followed by acid washing)	Distorted graphitic structure with nanopores	POD	Enzyme-cascade sensing colorimetry	Detection of acetylcholine (biomarker for Alzheimer's)	Mimics <i>Horse-radish peroxidase</i> has a significant sorbent assay used in early Alzheimer's detection	P-doping	Accurate detection limit $-0.96 \mu\text{m}$	42
Pt/CeO <sub>2</sub> (SAC)	Pt	3.42%	CeO <sub>2</sub> clusters with neutrophil-like cell membranes	Aqueous phase synthesis	Distinct core-shell with FCC fluorite structure of CeO <sub>2</sub> clusters	CAT	Scavenges ROS, reduces neuroinflammation, and mitigates the progression of brain diseases (Mitophagy)	Brain diseases and cancer therapy	Potential to cross the blood-brain barrier and target dopaminergic neurons; Higher number of oxygen vacancies (57.11%)	—	Scavenging rate $-91.15\%$ for $\bullet\text{OH}$	43
Fe-N <sub>x</sub> SANs (SAN)	Fe	0.41%	Fe-doped polypyrrole (PPy) nanotubes	Pyrolysis ( $N_2$ atm) followed by acid leaching	Distorted graphitic layers in Fe-N <sub>x</sub> SANs	HRP and POD	Fenton-like reaction	Early detection of A $\beta$ 1-40, a biomarker of Alzheimer's	Ultra-low LOD of $-0.88 \text{ pg mL}^{-1}$ ; SAN-LISA over ELISA (LOD $-9.98 \text{ pg mL}^{-1}$ ); Max atom utilization	—	LOD $-0.88 \text{ pg mL}^{-1}$	44
FeMn DSAs/N-CNTs (SAN)	Fe and Mn	Can be optimized	N-doped carbon nanotubes	Pyrolysis-acid etching; at $900 \text{ }^\circ\text{C}$ , 1 h @ $5 \text{ }^\circ\text{C min}^{-1}$ in $N_2$ atm	Dual single atoms dispersed on N-doped CNTs	POD	Colorimetry	Detection of acetylcholinesterase (AChE) and its inhibitor (huper-zinc A); Brain disease treatment	Simple and rapid activity monitoring, unlike inhibitor (huper-zinc A); Brain disease treatment	Interference from other analytes not monitored	LOD $-0.066 \text{ U L}^{-1}$ (AChE) LOD $-4.17 \text{ nM}$ (Inhibitor)	45
Rh-N/C	Rh	—	Carbon dots	Pyrolysis	Rugged rhombic dodecahedron	OXD, SOD	Colorimetry	Detection of acetylcholinesterase (AChE)	Better linear response and stability	—	LOD $-3.2 \times 10^{-4} \text{ mU mL}^{-1}$	46
MitoCAT-g (SAC)	Au	0.5 wt%	Carbon dots	Heating-precipitation-fabrication	Rod or line-like distribution pattern in cells in mitochondria	OXD	Depletes GSH and elevates ROS in mitochondria	Apoptosis-based cancer therapy	Disrupts redox homeostasis, amplification of oxidative stress	—	Max survival rate $-87.5\%$ (after 62 days)	47
Au-CeO <sub>2</sub> (SAC)	Au	0.3 Au adjacent oxygen and thus generates more oxygen vacancies	Chloroauric acid ( $0.5 \text{ mmol L}^{-1}$ )	Calcination (at $200 \text{ }^\circ\text{C}$ for 4 h)	Fluorite-type FCC structure	—	Biosensing	Detection of $H_2O_2$ released from pulmonary carcinoma cancer cells (A549)	Good reproductibility $-RSD 2.2\%$ Highly selective $-$ no significant response to interfering substances, like dopamine or ascorbic acid in amperometry	—	Excellent detection limit $-1.4 \text{ nM}$	48

Table 1 (continued)

SAC/ SAzymes	Metal/Active site	Metal loading (wt%)	Supporting precursor	Synthesis	Structure	Enzymatic activity	Catalytic mechanism	Applications	Advantages and practical implication	Limitations	Efficiency	Ref.
Cu/TiO <sub>2</sub> (SAC)	Cu	7.06%	SiO <sub>2</sub> nanoparticles coated with TiO <sub>2</sub> , adsorbing Cu precursor onto the TiO <sub>2</sub> layer	Reformative wrap-bake-strip Temperature and reaction conditions – Calcination – 900 °C Etching – alkaline medium	Single Cu atom anchored on the most stable Ti vacancies of low TiO <sub>2</sub> sonosensitizers	POD	(Fenton-like reaction) H <sub>2</sub> O <sub>2</sub> into •OH	Nano-Sono sensitive for triple negative breast cancer (TNBC)	Excellent alternative to sonosensitizers not addressed	Potential resistance mechanism	Tumour inhibition rate – 70.35%	inhi-49
Co-N <sub>4</sub> -C (SAN)	Co	0.506 wt%	N-doped porous carbon	Coordination-pyrolysis-corrosion	Co atoms four-coordinated by N atoms	Catalase lowered by N OXD	H <sub>2</sub> O <sub>2</sub> decomposition into O <sub>2</sub> followed by cytotoxic O <sub>2</sub> <sup>•-</sup> formation	Tumour-specific treatment via Cascade reactions.	Reduces side effects in malignant tumours	—	Tumour inhibition rate – 66% (SAC alone)	inhi-50
FeN <sub>5</sub> (SAN)	Fe	—	Zeolitic imidazole framework-8 (ZIF-8)	Temperature and reaction conditions – 900 °C under N <sub>2</sub> atmosphere	Polyhedral structure with collapsed planes	Struc-POD	H <sub>2</sub> O <sub>2</sub> into toxic •OH	Antitumor effect	Superior POD and catalytic efficiency – 7.64 and 3.45 × 10 <sup>5</sup> times higher than the traditional Fe <sub>3</sub> O <sub>4</sub> nanozyme	—	Tumour inhibition rate – 91.9%	inhi-51
S-N/Ni (SAN)	Ni	0.96%	NiCo Prussian blue analogue (NiCo PBA) nanocubes	Calcination Temperature and reaction conditions – 500 °C for 2 h under an Ar atmosphere	An edge-rich S and N dual heteroatom-incorporated on a Ni single-atom enzyme (S-N/Ni SAE)	GSHox – and POD	Fenton-like reaction	Ferroptosis-based tumour therapy	Inactivates glutathione peroxidase 4 and induces lipid peroxidation	—	Tumour inhibition rate of S-N/Ni PSAE – 49.87%	inhi-52
Cu SAs/CN (SAN)	Cu	At 90 minutes – 0.48 wt%	Graphitic carbon nitride (g-C <sub>3</sub> N <sub>4</sub> )	Electrochemical deposition	Irregular ultrathin-layer porous	Ascorbate peroxidase (APX)	Anti-oxidative damage	APX alternative for regulating intracellular H <sub>2</sub> O <sub>2</sub> levels & protecting cells from oxidation stress	Cell viability of HeLa cells maintained at more than 90%	—	High catalytic efficiency (k <sub>cat</sub> /K <sub>m</sub> = 1.60 × 10 <sup>4</sup> mm <sup>-1</sup> s <sup>-1</sup> )	53
BSA-Cu SAN (SAN)	Cu	5.4 wt%	BSA (bovine serum albumin)	Wet chemistry	Cu is atomically coordinated with N and O atoms in BSA-Cu SAN, forming a structure of CuN <sub>2</sub> O <sub>2</sub>	ROS generation	Anti-tumour in colorectal cancer (Fenton-like reaction) H <sub>2</sub> O <sub>2</sub> into •OH	Destroy pathogen (F. nucleatum)-tumour symbionts	Depletes glutathione (GSH), leading to the apoptosis of cancer cells	—	Tumour inhibition rates: Intratumoral – 82.97% Intravenous – 76.63%	inhi-54
HNTMs-Au (SAC)	Au	Au-N <sub>1</sub> -ppy 0.07%	Zirconium porphyrinic MOF	Solvothermal method	Au atom is coordinated with four N atoms	Chlorophyll mimic	Consistent light-induced positive shifts in potential	Photo-coupled electrocatalysts	Ultrahigh turnover frequency	Low metal loading capacity	Turnover frequency –	55,56

Table 1 (continued)

SAC/ SAzymes	Metal/Active site	Metal loading (wt%)	Supporting precursor	Synthesis	Structure	Enzymatic activity	Catalytic mechanism	Applications	Advantages and practical implication	Limitations	Efficiency	Ref.
Pd-N-C (SAN)	Pd	0.18 wt%	hollow nanotubes	Top-down strategy-pyrolysis Temperature and reaction conditions –900 °C for 3 h under N <sub>2</sub> atmosphere	and anchored in the centre of a square-planar porphyrin unit	POD and GSHOX	Promotes ferroptosis by the upregulation of lipid peroxides and ROS	Ferroptosis-boosted photothermal therapy	CO <sub>2</sub> selective reduction and renewable energy Can cleave stress-induced heat shock proteins (HSPs)	—	37 069 h <sup>-1</sup> at 1.1 V CO faradaic efficiency (FE) – 94.2% at 0.9 V Photo-thermal conversion efficiency – 33.98%	57
Fe50-N-C-900 (SAC)	Fe-N-C	0.15%	MOF (ZIF-8), with the addition of a certain amount of Fe(NO <sub>3</sub> ) <sub>3</sub>	Pyrolysis temperature – 900 °C graphitic N as dominant species	Contains pyridinic N and graphitic N as dominant species	POD	Biosensing	Fuel cells, batteries	Cost-effective metal alternative for oxygen reduction reaction (ORR), pH independent	Biomedical application is still yet to be explored	Onset potential – 1.00 V Half-wave potential – 0.92 V, which is greater compared to N-C-900 and PtC, indicating its superior performance Inhibition rate – 99.87%	58
PMCSs Nanozymes in combination with Zn (SAC)	Zn	3.12 wt%	Zinc-based zeolitic-imidazolate framework (ZIF-8)	(mSiO <sub>2</sub> ) <sub>x</sub> protected pyrolysis at 800 °C	Uniform size distribution with atomically dispersed zinc	POD	Antibacterial effect	Wound healing	Inhibits the growth of <i>Pseudomonas aeruginosa</i> bacteria	—	—	59
Cu-N-C (SAN)	Cu	—	CuCl <sub>2</sub> and KCl	Wet chemistry	Elemental distribution of Cu, N, and C in Cu-N-C in nanosheets	POD, OXD	Antibacterial therapy (•OH) and (O <sub>2</sub> • <sup>-</sup> )	Wound healing	Antibacterial effect	—	Inhibition rates: <i>P. aeruginosa</i> – 71.4% <i>S. aureus</i> – 82.8%	60
Fe-N-C (SAN)	Fe	—	Zinc-based zeolitic-imidazolate framework (ZIF-8)	Wet chemistry and high-temperature calcination	Large mesoporous spherical structure	POD	Fenton-like catalysis (H <sub>2</sub> O <sub>2</sub> to •OH)	Antibacterial via photothermal treatment enhanced area – 413.9 m <sup>2</sup> Wound healing	Large pore size – 4.0 nm, high specific surface content	Lower metal atom content	K <sub>m</sub> = 4.84 mmol L <sup>-1</sup> Photo-thermal efficiency of SAzyme – 23.3%	61
CuSA C <sub>6</sub> N <sub>6</sub> (SAC)	Cu	2.36 wt%	Dicyandiamide-Cu complex	Microwave-assisted condensation	Uniformly dispersed single-atom copper	POD	Biosensing	Glucose biosensors	Inhibits negative interferences (electron transfer b/w Cu-N	—	LOD – 15.07 mM (normal mode)	62

Table 1 (continued)

SAC/ SAzymes	Metal/Active site	Metal loading (wt%)	Supporting precursor	Synthesis	Structure	Enzymatic activity	Catalytic mechanism	Applications	Advantages and practical implication	Limitations	Efficiency	Ref.
DA-CQD@Pd (SAN)	Pd	Catechol-quinone redox and Pd single atoms	Catecholic carbon-quantum-dot (CQD)	<i>In situ</i> synthesis	DA-CQD@Pd SAN and immune adjuvant CpGODN into a hydrogel network	POD	Fenton-like reaction	Hydrogel-based catalytic immunotherapy	Quantum dots as supports instead of C-supports avoids aggregation	—	LOD – 1.20 mM under irradiation at 30 and 50 mWcm <sup>2</sup> Survival comparison rate – over 75%	com-63
Mn-N-C (SAN)	Mn-N	—	N-doped porous carbon & ZIF-8	Etching-adsorption – pyrolysis – 900 °C, Ar atmosphere	Mn atoms trapped in N-rich porous carbon	Oxidase and peroxidase	Fenton-like reaction O <sub>2</sub> to cytotoxic CO <sub>2</sub>	Enzymatic therapy, provides synergistic effect for tumour treatment	Disrupts redox hemostasis in tumour cells PEGylation increases stability of SAC	Metal loading capacity not mentioned	23.1% Cell proliferation reduction – 58%	64
OxgeMC-C-Ru (SAN)	Ru-O6	Loading ratio – 2.18 wt% High capacity for the photosensitizer Ce <sub>6</sub>	Mn <sub>3</sub> [Co(CN) <sub>6</sub> ] <sub>2</sub> metal-organic framework (MOF)	<i>In situ</i> multicomponent self-assembly	Coordination, hydrophobic, and electrostatic interactions among the organic linker, PVP polymer, photosensitizer, and metal ions	Catalase	Oxygen generation in the tumour microenvironment	Photodynamic therapy	<i>Solid tumour hypoxia</i>	—	Tumour inhibition rate – 90%	65
SA-Pt/g-C <sub>3</sub> N <sub>4</sub> -K (SAN)	Pt-N-C	3%	Pristine g-C <sub>3</sub> N <sub>4</sub> -K	Ionothermal method Temperature and reaction conditions – 150 °C for 2 h under Ar atmosphere	Planar-square configuration with Pt-N <sub>4</sub> sites composed of four-fold Pt-N coordination bonds	POD	Fenton-like reaction	H <sub>2</sub> O <sub>2</sub> detection and anti-bacterial therapy	High metal loading %	—	Bacterial killing efficiency of over 99.99% in the presence of H <sub>2</sub> O <sub>2</sub>	66
NCAGFe (SAN)	Fe-N <sub>4</sub>	0.95 wt%	N-doped porous carbon aerogel	Pyrolysis and acid etching – 900 °C, (97% Ar + 3% H <sub>2</sub> ) for 3 h	N-doped porous carbon aerogel with atomically dispersed Fe atoms within carbon matrix-Hierarchical pore structure	GO <sub>x</sub> and HRP	Oxidation of o-phenylenediamine to 2,3-diaminophenazine in the presence of H <sub>2</sub> O <sub>2</sub>	Glucose detection	Excellent reproducibility, stability, cost effectiveness	—	LOD – 3.1 μM (fluorometric assay) LOD – 0.5 μM (electrochemical detection)	67

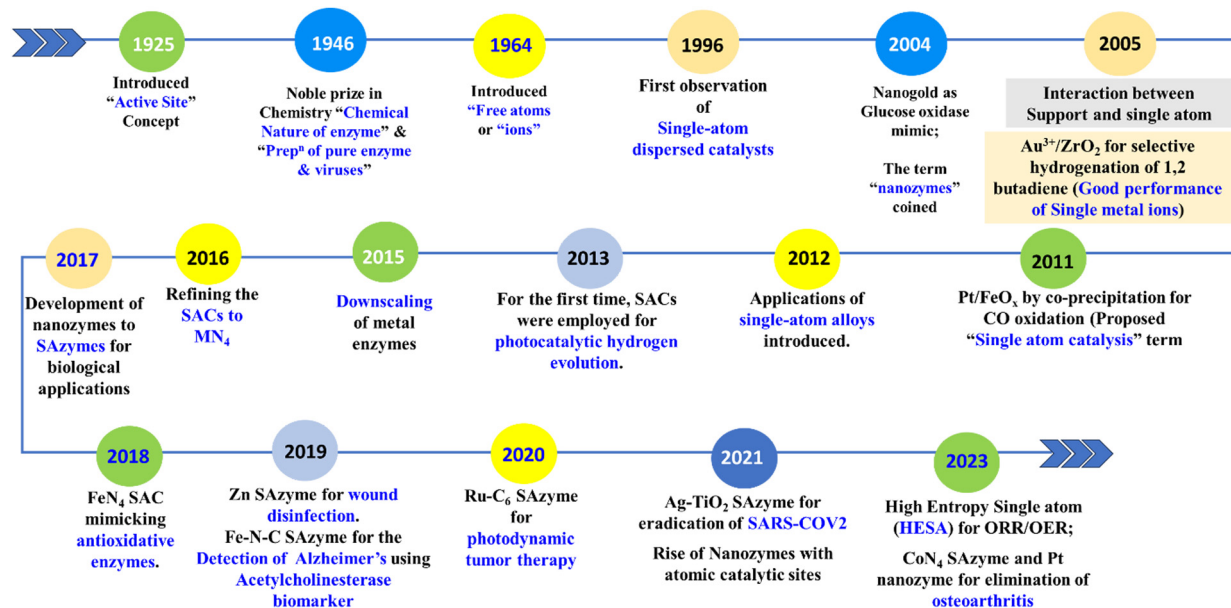


Fig. 1 The development of SACs and SAzymes over the years in various fields of applications.<sup>38,88–95</sup>

reduced stability of atomically dispersed atoms when exposed to high temperatures. Consequently, achieving stable SACs at metal loadings suitable for practical applications is a challenging task.<sup>84–86</sup>

Initially, Wu *et al.* in 2022,<sup>87</sup> chose Ni-SAC as a representative model to illustrate our approach for fabricating M-SACs with adjustable mesoporous architectures. The synthesis of Ni-SAC involved a three-step procedure (depicted in Fig. 1a(i)). First, various SiO<sub>2</sub> hard templates, such as SiO<sub>2</sub> nanoparticles (SiO<sub>2</sub>-NPs), Santa Barbara Amorphous-15 (SBA-15), or Mobil Composition of Matter no. 48 (MCM-48), were introduced into an aqueous solution containing NiCl<sub>2</sub> and *o*-phenylenediamine (*o*PD). Subsequently, ammonium peroxydisulfate ((NH<sub>4</sub>)<sub>2</sub>S<sub>2</sub>O<sub>8</sub>) was utilized to complete the polymerization of *o*PD, resulting in the formation of Ni-P*o*PD-SiO<sub>2</sub> composites. Finally, the composites underwent pyrolysis, followed by NaOH and H<sub>2</sub>SO<sub>4</sub> etching steps, yielding three distinct types of Ni-SACs: Ni-SAC/SiO<sub>2</sub>-NPs, Ni-SAC/SBA-15, and Ni-SAC/MCM-48. Although we anticipated similar Ni atomic arrangements, the utilization of different hard templates led to varying microscopic architectures and mass diffusion behaviours in the resulting Ni-SACs, as illustrated in Fig. 1a(ii), (iii).

Another method was reported by Fan *et al.* in 2016,<sup>96</sup> whose group worked on the synthesis and characterization of an A-Ni-C catalyst, which allowed obtaining well-dispersed Ni metal within a graphitized carbon matrix using an electrochemical corrosion process. Initially, a Ni-based metal-organic framework (Ni-MOF) served as the precursor (Fig. 1b). Subsequent to carbonization at 700 °C in a nitrogen (N<sub>2</sub>) atmosphere, Ni nanoparticles encapsulated within graphene layers (Ni@C) were generated. To remove excess Ni metal, a hydrochloric acid (HCl) leaching treatment was employed, resulting in HCl-Ni@C. Following the HCl treatment, hollow onion-like carbon nanoshells remained, accompanied by residual Ni nanoparticles protected

by graphene layers. Subsequently, electrochemical cyclic-potential was applied to the HCl-Ni@C catalyst-decorated electrode, leading to an unexpected activation process.

Zeolite, metal-organic frameworks (MOFs), graphene, and carbon nitride (CN) materials are commonly utilized for synthesizing isolated atoms, with the confinement strategy being a widely employed method for controlling the positioning of single atoms. "Confining" refers to the process of coordinating single atoms with substrates *via* covalent bonds, while maintaining their coordinatively unsaturated state to act as active centres.<sup>97,98</sup> This approach effectively stabilizes single atoms and prevents their migration during processes. Typically, this strategy involves two steps. Initially, metal precursors are encapsulated within porous materials, and subsequently, isolated metal atoms anchored on the substrate are obtained by eliminating the residual precursors. For example, Wu and colleagues<sup>99</sup> devised a method for synthesizing atomically dispersed Mn-N-C catalysts through a two-step doping and adsorption strategy. In the initial doping phase, Mn-doped ZIF-8 underwent acid leaching to yield a partially graphitized carbon host with nitrogen co-doping and porous structures. In the subsequent adsorption step, additional Mn and nitrogen sources were introduced and absorbed into the carbon host alongside Mn-NC first powder. Thermal activation was then employed to generate MnN<sub>4</sub> sites with increased density. This catalyst demonstrated promising activity and enhanced stability for the oxygen reduction reaction (ORR).

Efforts to synthesize stable SACs at high temperatures have expanded beyond traditional wet-chemistry methods. Directly converting metal nanoparticles into single atoms is crucial for both research and practical applications. Zhang *et al.* achieved this by redispersing Pt nanoparticles to form a high-loading and thermally stable SAC through a strong covalent metal-support interaction (CMSI). The process involved the ethylene

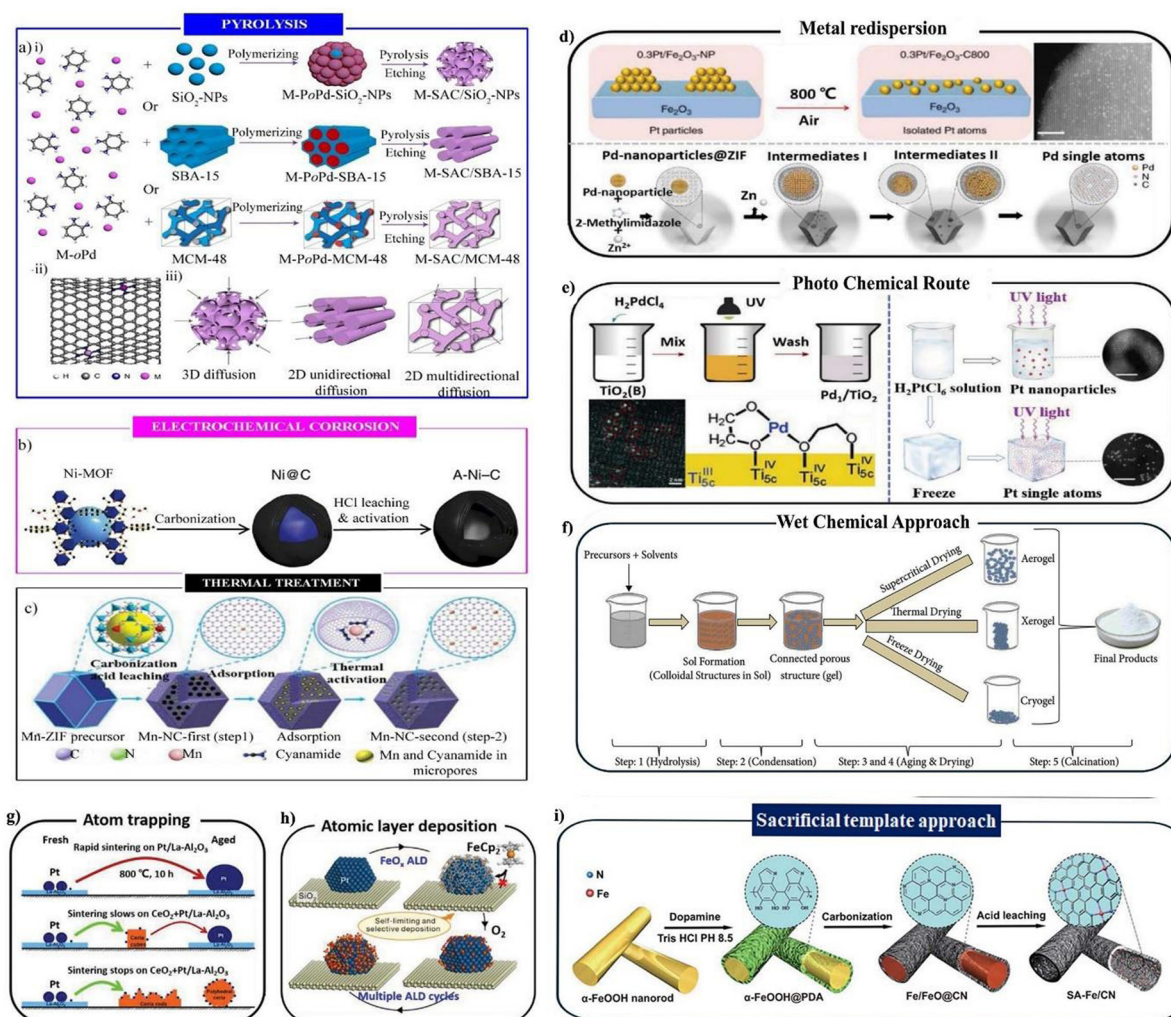


**Fig. 2** Various synthesis techniques for SACs/SANs. (a) Synthesis strategy of a family of M-SACs (M = Ni, Co, Mn, Zn, Cu, Sc and Fe) as well as multi-M-SACs including binary, ternary, quaternary and up to seven different metal centres. Reproduced with permission.<sup>87</sup> Copyright 2022, Nature. (b) Schematic of the synthesis and activation processes of Ni–C catalysts. The Ni–MOF used as a precursor consisted of an orthorhombic crystal. Atoms are shown as follows: C, black; H, white; O, red; N, blue; and Ni, royal blue. Reproduced with permission.<sup>96</sup> Copyright 2016, Nature; (c) fabrication of Pt<sub>75</sub>-SAzyme using ZIF-8. Reproduced with permission.<sup>99</sup> Copyright 2018, the Authors, published by Springer Nature; (d) and (e) diverse synthesis methods studied to prepare SACs: (d) atom trapping strategy; (e) transformation of nanoparticles to single atoms. Reproduced with permission.<sup>100</sup> Copyright 2022, Wiley. (f) Schematic of the different stages of the sol–gel process: from precursor to aerogel. Reproduced with permission.<sup>101</sup> Copyright 2021, Hindawi. (g) Atomic layer deposition process. Reproduced with permission.<sup>102</sup> Copyright 2016, American Association for the Advancement of Science. (h) Photochemical reduction route. Reproduced with permission.<sup>103</sup> Copyright 2019, Springer Nature. (i) Schematic of the synthesis of SA-Fe/CN. Reproduced from ref. 104 with permission. Copyright 2017, American Chemical Society.

glycol reduction of Pt nanoparticles, deposition onto Fe<sub>2</sub>O<sub>3</sub>, and calcination at 800 °C in flowing air.

Similarly, Li *et al.* observed that noble metal nanoparticles (Pd, Pt, Au) could convert into thermally stable single atoms on nitrogen-doped carbon (CN) substrates. They utilized nitrogen defects on CN to capture and anchor the metal atoms. The synthesis involved mixing nanoparticles and Zn(NO<sub>3</sub>)<sub>2</sub> with a 2-methylimidazole solution to grow ZIF-8 crystals on the metal nanoparticles. Subsequent heating to 900 °C under flowing nitrogen gas resulted in the conversion of metal–metal bonds into metal–N bonds, yielding individual atoms. This redispersion strategy proved effective for both oxide and CN supports under inert atmospheres (Fig. 2a).

Despite the significant advancements made, achieving a high loading of isolated metal atoms remains challenging in synthesis. Photochemical reduction, which involves the adsorption of photons and electronically excited states, has emerged as a promising method for synthesizing isolated metal catalysts. Notably, groups led by Flytzani-Stephanopoulos and Zheng have successfully fabricated atomically dispersed catalysts using this method.<sup>105,106</sup> Zheng's group achieved a high loading of single Pd atoms (up to 1.5%) on ultrathin TiO<sub>2</sub> substrates. The synthesis process involved dispersing H<sub>2</sub>PdCl<sub>4</sub> solution into TiO<sub>2</sub> nanosheets followed by UV treatment and subsequent centrifugation and washing. The atomic dispersion of Pd species was confirmed by aberration-corrected STEM.

Ethylene glycolate (EG) radicals played a crucial role in the formation mechanism of the catalysts.

Additionally, Wu and colleagues demonstrated that Pt single atoms can be dispersed on various substrates, including carbon-based materials and ZnO nanowires, through an iced-photochemical reduction process. Single Pt atoms were stabilized *via* Pt–C or Pt–O coordination, as confirmed by X-ray absorption fine structure (XAFS) analysis (Fig. 2b).<sup>107</sup> The photochemical strategy offers simplicity and time-saving advantages over traditional wet-chemistry methods, presenting a promising route for preparing SACs.

The enduring stability and chemical activity of individual atom species residing on supportive surfaces ultimately hinges on their electronic configuration. This configuration can be substantially adjusted by the specific binding environment in which they find themselves. It is important to note that single-atom catalysis is not solely attributable to the single metal atom itself, rather, it encompasses the interactions with its surroundings. These interactions can be likened to the metal–ligand interactions observed in homogeneous catalysis. Furthermore, single-atom species can also assume roles as promoters, even if they do not directly participate in the catalytic reactions.<sup>108–110</sup>

The catalyst's stability decreases as the thickness of the amorphous layer is reduced. This indicates that the combined influence of the amorphous and crystalline components imparts high stability to the catalyst. Amorphous substances, such as layered double hydroxides (LDHs), offer many unsaturated coordination sites. These characteristics are advantageous for immobilizing single atoms by enhancing their interactions with the substrate. Nevertheless, it is important to highlight that amorphous materials generally exhibit lower stability when subjected to highly corrosive and oxidative conditions, especially when compared to their crystalline counterparts. Consequently, there is a strong interest in developing hybrid materials that merge the qualities of amorphous and crystalline LDHs. The goal is to strike a balance that enhances both the stability and activity simultaneously.<sup>111,112</sup>

Zhang *et al.* further confirmed the inherent stability of single-site Pt catalysts used for CO oxidation. In their experiments, they found no noticeable deactivation even after subjecting the catalyst to 60 consecutive cycles at temperatures ranging from 100 °C to 400 °C. The remarkable stability of this catalyst was attributed to the Pt atoms being firmly attached to the inner surface of the mesoporous Al<sub>2</sub>O<sub>3</sub> substrate. These Pt atoms were suggested to be stabilized by coordinate

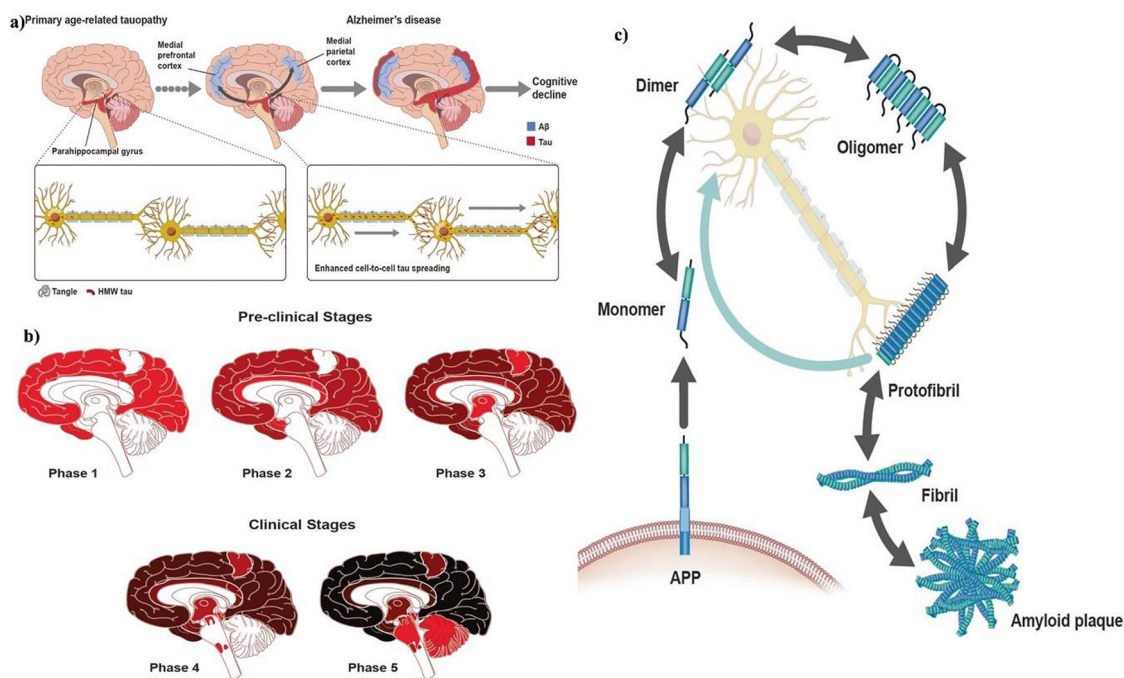


**Fig. 3** (a) Evidence-driven experimental model of A $\beta$ -tau synergy. In the neocortical regions of Alzheimer's disease patients' brains, tau (red) and amyloid plaques (blue) constituted of amyloid- $\beta$  accumulate at the same time, promoting tau propagation across neocortical regions dependent on amyloid- $\beta$ . Tau (bottom) inter-neuronal spreading is amplified in AD brains with plaque accumulation and tangle accumulation. Adapted with permission from ref. 124. (b) Traditional neuropathological phases of amyloid- $\beta$  deposition in Alzheimer's disease dementia. Red areas in Phase 1 depict the cortical regions with the initial accumulation of amyloid- $\beta$  during the early pre-clinical stage. Continued deposition in the same areas is shown in darker colors in the subsequent stages, with the new areas showing amyloid- $\beta$  in red in each phase. Neocortical regions with the early accumulation of amyloid- $\beta$  in phase 1 include association cortices. Additional accumulation is seen in the allocortical regions and midbrain (phases 2 and 3), with the cerebellum and brain stem having amyloid- $\beta$  accumulation in the late-phase clinical stages. The change to darker shading indicates the continuous accumulation of A $\beta$ . Adapted with permission from ref. 125. (c) Amyloid- $\beta$  aggregation species and evidence of reversible states: the amyloid- $\beta$  cycle. The aggregation species of A $\beta$  can exist as monomers, dimers, oligomers, protofibril, fibril and amyloid plaques. These species exist in the steady state where one form can convert to another in a bidirectional manner. The species are characterized by the aggregate size, conformation state and solubility, with fibril and amyloid plaque being insoluble. Adapted with permission from ref. 126.

unsaturated pentahedral  $\text{Al}^{3+}$  centres. There is broad consensus that the performance, specificity, and durability of SACs can be fine-tuned by altering how the anchored atoms interact with the supporting surfaces. The precise positioning of these metal atoms on the support surface is thought to determine the intensity of their interactions with the support material. Within these catalytic systems, the solitary metal atoms typically affixed to cationic vacancies, equivalent cationic positions, or other surface imperfections on the support, are recognized as the active sites.<sup>113</sup>

## 4. Role of SACs/SAzymes in Alzheimer's detection

Alzheimer's disease (AD) stands as the most common type of dementia. Globally, dementia affects approximately 47 million individuals, with 60–80% of these cases being attributed to AD.<sup>114,115</sup> This suggests that the prevalence of dementia will surpass 100 million by 2050. The cellular phase of AD occurs simultaneously with the accumulation of amyloid  $\beta$  in the brain, triggering the propagation of tau pathology, as shown in Fig. 2. Over 40 genetic risk loci linked to AD have already been identified, with apolipoprotein-E (APOE) alleles demonstrating the strongest connection with the disease. Emerging biomarkers, like plasma assays, and PET scans targeting phosphorylated tau and amyloid  $\beta$  show indicative potential for both clinical and research applications. Promising pharmacological treatments, like those targeting anti-tau, and anti-inflammatory mechanisms, and anti-amyloid  $\beta$  are in advanced stages of clinical trials.<sup>116–118</sup> AD is characterized by a gradual decline in episodic memory followed by cognitive impairment. In recent times, microbial agents have gained attention as potential contributors to AD's origin, particularly periodontal pathogens causing periodontitis (Pd), a condition linked to increased risks of atherosclerosis, adverse cognitive outcomes, cardiovascular events, and diabetes.<sup>119</sup> Pd affects 20% to 50% of older adults, initiated by periodontal bacteria, such as *Treponema denticola*, *Aggregatibacter actinomycetemcomitans*, *Porphyromonas gingivalis*, and *Tannerella forsythia*. These bacteria trigger gingival inflammation, the destruction of connective tissue, the formation of periodontal pockets, the loss of alveolar bone, and eventual tooth loss. Multiple potential pathways connecting Pd to AD have been proposed, encompassing brain infiltration by Gram-negative bacteria present in dental biofilms, the release of bacterial by-products into the brain through bloodstream invasion, and direct impacts on peripheral nerves.<sup>120,121</sup> Amyloid beta 1-40 ( $\text{A}\beta$  1-40), abundant in the human body (ranging from several tens to several hundreds of picograms per millilitre), readily aggregates into insoluble toxic forms, serving as a key neuropathological indicator for AD. The early detection of  $\text{A}\beta$  1-40 can therefore provide valuable insights into estimating the risk or early-stage presence of AD.<sup>122,123</sup> The prevailing model in AD suggests that the pathophysiology of  $\text{A}\beta$  may be an upstream pathophysiological event and could act as a trigger or facilitator of downstream molecular pathways leading to

cortical neurodegeneration, such as tau misfolding, tau-mediated toxicity, tangle accumulation, and tau spreading (Fig. 3a). Biomarker-based observations and experimental research showing a temporal  $\text{A}\beta$ -tau synergy, where a pathophysiological sequence exists between tau-mediated toxicity and  $\text{A}\beta$  aggregation, are supported by genetic investigations.<sup>124</sup>

Quantitative neuroimaging investigations have confirmed neuropathological studies that show a spatial-temporal evolution of brain  $\text{A}\beta$  accumulation. This accumulation starts in cerebral regions (like association cortices), where the neuronal populations have high rates of metabolic bio-energetic activity. It then moves from the neocortex to the allocortex to the brainstem and ultimately to the cerebellum (Fig. 3b).<sup>125</sup> Once soluble monomers are produced,  $\text{A}\beta$  can exist in many intermediate aggregation states, such as dimers and trimers, soluble oligomers, and protofibrils. Eventually, it forms fibrils that collect in plaques, which are commonly considered a neuropathological characteristic of AD (Fig. 3c). From a diagnostic and therapeutic standpoint, it is critical to comprehend the biology, interconnected dynamics, and bioactivity of these intermediate assemblies under both normal and pathological settings.<sup>126</sup>

SACs, a subtype of nanozymes, are composed of individual metal atoms dispersed on a supportive surface. These single-atom nanozymes have attracted significant attention in the realm of bio-catalysis.<sup>127</sup> This is attributed to their durability, exceptional catalytic prowess, and a distinctive attribute – the maximum utilization of each atom (Fig. 2d–f). An innovative high-density Fe- $\text{N}_x$  single-atom peroxidase-like nanozymes (Fe- $\text{N}_x$  SANS) system was presented by Zhaoyuan *et al.*, 2020, who used a nanoconfined strategy involving pyrolyzed polypyrrole (PPy) nanotubes for the detection of  $\text{A}\beta$ 1-40, revealing better thermal and pH stability in the Fe- $\text{N}_x$  SANS. Herein, the Fe- $\text{N}_x$  SANS produced could catalyze the conversion of  $\text{H}_2\text{O}_2$  into hydroxyl radicals through a Fenton reaction, demonstrating excellent peroxidase-like activity.<sup>44</sup> Nevertheless, deviations in dopamine levels, either excessive or deficient, bear additional consequences, potentially contributing to the onset of conditions, such as AD.<sup>128</sup> A novel approach involving pyrolytically Au-enhanced copper single-atom catalysts for the real-time electrochemical detection of dopamine in neuronal cell and geriatric plasma was presented by Gayathri *et al.*, 2023, with high sensitivity, structural stability, and biocompatibility. The fabricated electrodes were based on single copper and gold atoms anchored on bioinspired chitosan-extracted carbon (CuAu SACs/BC).<sup>129</sup> In contrast to traditional nanozymes, SACs are typically composed of isolated, positively charged metal atoms that are stabilized by coordination with surrounding atoms or ligands. This coordination prevents the metal atoms from clustering together and allows the formation of distinct metal-support interactions, rather than direct metal-metal bonds. This structural difference enhances their catalytic activity and selectivity by exposing individual metal atoms for more efficient catalytic processes (as depicted in Fig. 2g–i). This makes them applicable as sensing materials, enabling amplified signals and the sensitive detection of biomolecules. The distinctive electronic and geometric characteristics of SACs

Table 2 Different catalysts used for the detection of Alzheimer's biomarkers

Catalyst	LOD	Active biomarker	Catalyst synthesis technique	Michaelis-Menten constant (KM)	Mode of mechanism	Precursor	Catalytic radicals	Linear range	Advantages	Ref.
Fe-N-C	0.88 pg mL <sup>-1</sup>	Aβ 1-40	Pyrolyzed polypyrrole (PPy) nanotube <i>via</i> a nanoconfined strategy	17.12 mM	Catalyzes H <sub>2</sub> O <sub>2</sub> to generate hydroxyl radicals <i>via</i> a Fenton reaction, which can be recognized as a superior peroxidase-like activity	Derived from Fe-doped polypyrrole nanotubes	•OH	1–2000 pg mL <sup>-1</sup>	Higher sensitivity, better thermal and pH stable catalytic properties	44
Fe-N-C	1.9 pg mL <sup>-1</sup>	Acetylcholinesterase	Pyrolysis	0.129 mM	—	Fe atomic clusters on N-doped porous carbon	•O <sup>2-</sup>	0.005–50 ng mL <sup>-1</sup>	High catalytic efficiency	133
Fe-N-C	1.3 μM	Ascorbic acid	Pyrolysis	0.253 mM	Oxidase-like activity of Fe-N-C and colorimetric assay for GSH detection	Fe molecule trapped within ZIF-8	•O <sup>2-</sup>	1–10 μM	High sensitivity	134
Fe-N-C	0.014 mU mL <sup>-1</sup>	Acetylcholinesterase	—	1.81 mM	—	—	•O <sup>2-</sup>	—	High catalytic efficiency, low cost	135
Co-SAC	1.31 μM	Ascorbic acid	Pyrolysis	0.578 mM	Colorimetric assay	N-doped carbon and Co-doped graphitic carbon nitride	•O <sup>2-</sup>	0.3–2.5 U L <sup>-1</sup>	High catalytic efficiency and reactivity	136
Mo-SAN	0.12 μM	Choline	Cascade-anchored one-pot pyrolysis	0.044 mM	Colorimetric assay	2D N-doped carbon atom	•OH	0.5–35 μM	Stabilized molybdenum dispersion	137
FeMn-DSAs/N-CNTs	0.066 U L <sup>-1</sup>	Acetylcholinesterase(AChE)	Pyrolysis	0.86 mM	Colorimetric assay	N-doped carbon nanotubes	•OH	0.1–30 U L <sup>-1</sup>	High efficiency	45
Cu-N-C	0.60 ng mL <sup>-1</sup>	Acetylcholine	KCl-template strategy	19.94 mM	Colorimetric assay	N-doped carbon nanosheets	•OH	1–300 ng mL <sup>-1</sup>	High efficiency	138
Fe-SASC/NW	46.35 × 10 <sup>-9</sup> m	Hydrogen peroxide (H <sub>2</sub> O <sub>2</sub> )	Zinc-atom-assisted method	—	—	Doping single iron atoms in polypyrrole (PPy)-derived carbon nanowire	—	5.0 × 10 <sup>-10</sup> m to 0.5 m	High efficiency	139
Fe-SAs/NC	0.56 U L <sup>-1</sup>	Acetylcholinesterase (AChE)	—	—	—	N-doped porous carbon	—	2–70 U L <sup>-1</sup>	Rapid response, high sensitivity	140
Au-CeO <sub>2</sub>	1.4 nM	Hydrogen peroxide (H <sub>2</sub> O <sub>2</sub> )	—	—	—	Au catalyst loaded on CeO <sub>2</sub>	—	8 nM to 0.1 μM	Higher catalytic activity and selectivity	141

confer them with unique advantages, including improved atom utilization, reduced metal consumption, and augmented catalytic performance. Recently, SACs have emerged as a pioneering research frontier in catalysis-related domains. These catalysts consist of isolated metal atoms evenly dispersed on their substrates, showcasing exceptional catalytic activity and specialized catalytic sites due to their exceptional electronic structure, ample surface area, pathways for mass transfer, and optimal atom utilization. Furthermore, the active isolated metal atoms are firmly anchored within the support's crevices, imparting impressive stability even under adverse conditions. As a result of these distinctive attributes, SACs have attracted interest as

promising contenders for designing efficient single-atom nanozymes (SAzymes) tailored for biological sensing, tumour therapy, pollutant degradation, and more.<sup>130–132</sup> Table 2 list the key attributes of various catalysts used for the detection of Alzheimer's biomarkers. It includes details such as the name of the catalyst; its limit of detection (LOD), thus indicating its sensitivity; the active biomarker targeted; the technique employed for catalyst synthesis, thus offering insights into its fabrication process; the Michaelis–Menten constant (KM), thus indicating its affinity for the substrate and thus catalytic efficiency; the mode of mechanism, elucidating the chemical or biochemical process by which the catalyst interacts with the substrate; the

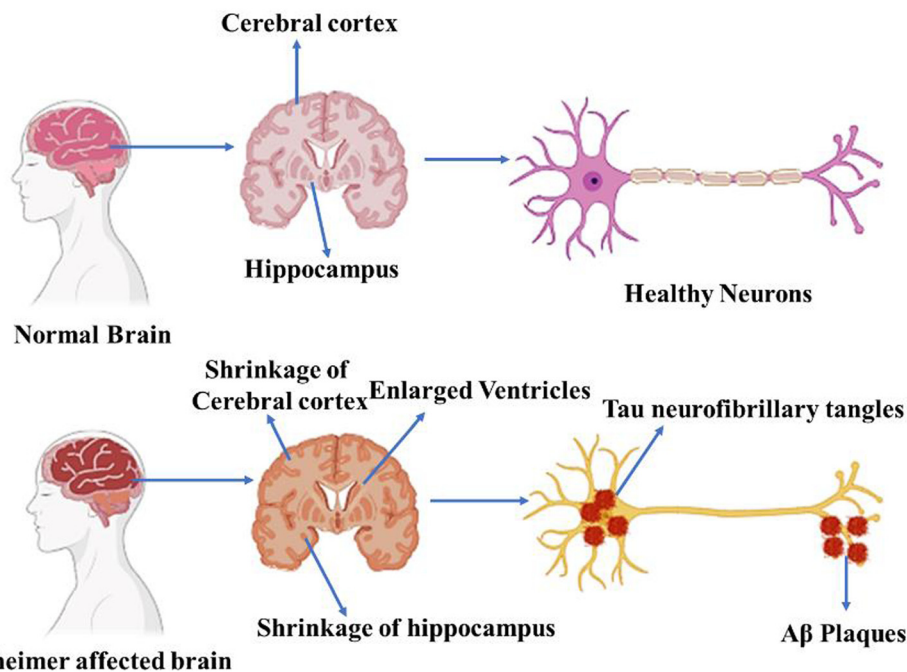


Fig. 4 Depiction of a healthy human brain vs. Alzheimer's-affected brain.

precursor material used in catalyst synthesis; the catalytic radicals generated during the reaction; the linear range, indicating the range of concentrations for reliable detection; and finally, its advantages specific to Alzheimer's detection, which may include enhanced sensitivity or stability. This comprehensive overview aids in comparing and evaluating the effectiveness of different catalysts in Alzheimer's biomarkers detection.

## 5. Mechanism of action

Acetylcholinesterase (AChE) is a requisite bio-enzyme present in the nervous system of living organisms. Fluctuations in the AChE concentrations may develop some neurodegenerative disorders (*e.g.* Parkinson's and Alzheimer's disease). It is an important monitoring indicator of stroke, cerebral infarction, and respiratory failure diseases. AChE catalyzes acetylcholine (ATCh) important for maintaining the functioning of the cholinergic nerves in the mammalian nervous system to acetic acid and thiocholine (TCh). Therefore, AChE has been used as an important biomarker for the detection of Alzheimer's disease, as depicted in Fig. 4. For this, pretreated human serum samples are treated with AChE solution at different concentrations. Also, 3,3',5,5'-tetramethylbenzidine (TMB), 2,2'-azino-bis (3-ethylbenzothiazoline-6-sulphonic acid) (ABTS) can be utilized as the chromogenic substrate.

The functionality resembling the peroxidase-like activity of a single atom was assessed using TMB as the chromogenic substrate. Upon the introduction of  $\text{H}_2\text{O}_2$ , the active site of the nanozymes facilitates the oxidation of TMB, resulting in the transformation of colourless TMB into blue ox-TMB. Meanwhile, AChE facilitates the hydrolysis of ATCh into acetic acid and TCh. TCh, which is generated in this process, leads to the reduction of

ox-TMB, consequently impeding TMB oxidation. The enzymatic function of AChE is noticeably hindered by an increase in the inhibitor Huperzine A (HA), resulting in reduced TCh production. Consequently, the presence of the enzyme enhances the catalytic oxidation of TMB. Initially, single-atom Fe sites uniformly cleave  $\text{H}_2\text{O}_2$  molecules to produce  $\cdot\text{OH} + \cdot\text{OH}$ . This leads to the subsequent formation of reactive  $\text{H}_2\text{O}$  molecules. Significantly, under acidic conditions,  $\cdot\text{O}$  reacts with  $\text{H}^+$  to generate  $\cdot\text{OH}$  on the single-atom sites, ultimately transferring to form stable  $\text{H}_2\text{O}$  molecules.<sup>45,142</sup>

## 6. SACs and SAzymes properties

SACs and SAzymes are emerging as promising tools in the diagnosis and treatment of AD. To be effective in these roles, SACs and SAzymes must possess specific properties tailored to the biochemical and pathological characteristics of AD. Below is an in-depth discussion of these properties.

### 6.1. High catalytic activity and selectivity

Amyloid beta 1-40 ( $\text{A}\beta$  1-40) is crucial for Alzheimer's detection but exists in low serum levels, requiring sensitive detection methods.  $\text{A}\beta$  accumulation is central to Alzheimer's pathology, forming neuritic plaques. In early-onset AD, genetic factors lead to excess  $\text{A}\beta$  production, while in late-onset AD, impaired clearance due to proteostasis failure causes plaque build-up.<sup>143</sup> SAzymes enhance immunoassays by providing high catalytic activity, stability, and maximum atomic utilization, surpassing traditional ELISA. SACs and SAzymes can potentially degrade these harmful aggregates, addressing key pathological indicators.<sup>44</sup> Additionally, selectivity is crucial to ensure that SACs and SAzymes target only the pathological substrates

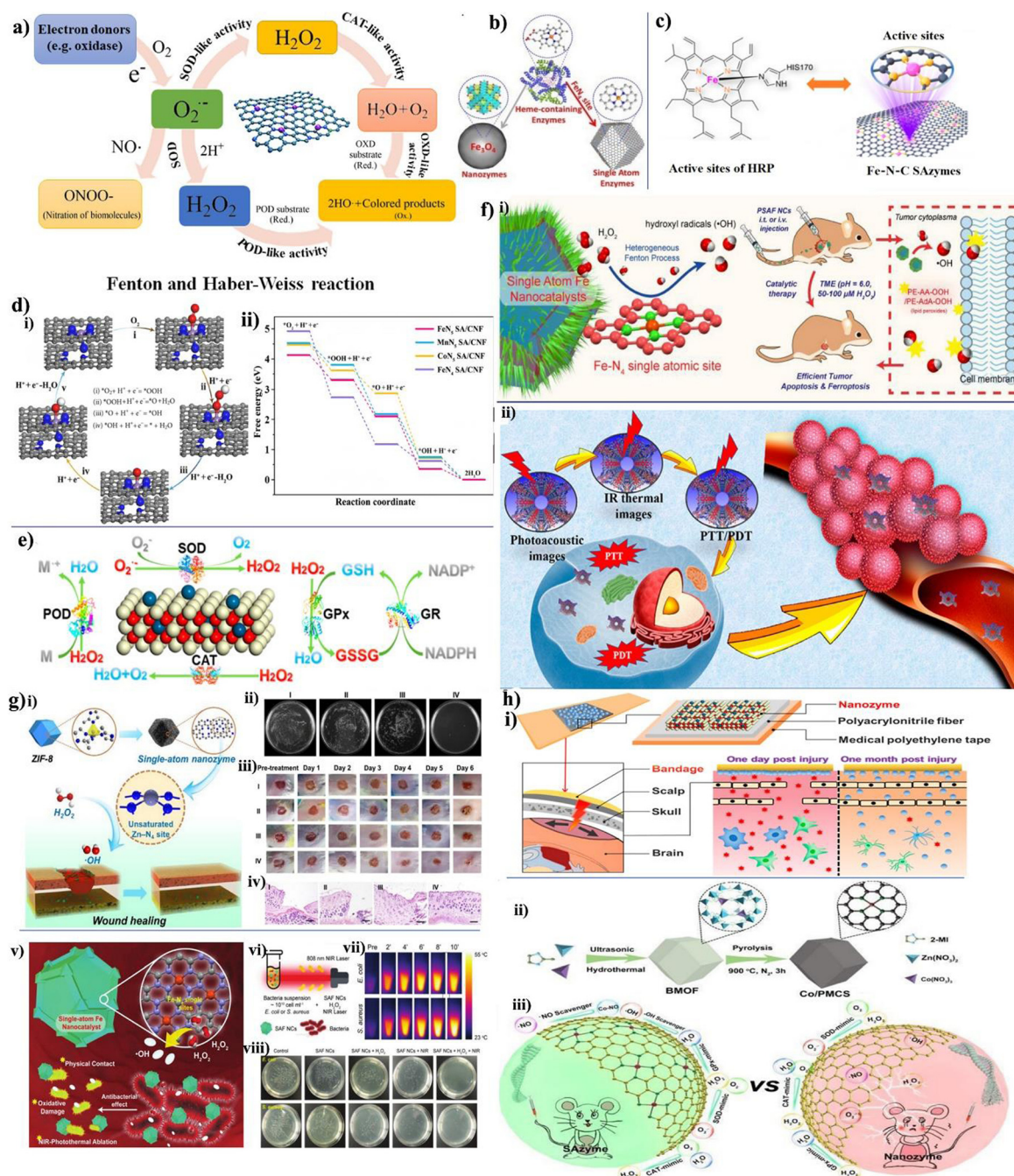


**Fig. 5** (a) Schematic exhibiting SAzymes with SOD-, POD-, and OXD-like activities. (b) Macrostructures and active sites of natural enzymes, nanozymes and Fe SAzymes. Reproduced with permission.<sup>155</sup> Copyright 2019, RSC. (c) Active sites of HRP and Fe-N-C SAzymes. Reproduced with permission.<sup>156</sup> Copyright 2019, ACS. (d) Theoretical investigation of oxidase-like activity over Fe<sub>5</sub> SA/CNF: (i) proposed reaction pathways of O<sub>2</sub> reduction to H<sub>2</sub>O with optimized adsorption configurations on Fe<sub>5</sub> SA/CNF, (ii) free energy diagram for oxygen reduction reaction on SAzyme mimics with TMB. Reproduced with permission.<sup>26</sup> Copyright 2019, Science Press. (e) Enzyme-mimetic properties of single-atom Pt/CeO<sub>2</sub> to mimic the first-line enzymatic antioxidant defence system.<sup>157</sup> Copyright 2019, ACS (f) (i) Nanocatalytic tumor therapy by SAzymes. Reproduced with permission.<sup>158</sup> Copyright 2019, ACS, (ii) schematic of NIR-stimulation of single-atom iron centers in P-MOF, resulting in efficient phototherapy via PDT and PTT, as well as PAL imaging. Reproduced with permission.<sup>159</sup> Copyright 2019, ACS. (g) (i) SAzymes for wound-healing applications, (ii) Photographs of bacterial colonies formed by *P. aeruginosa* after exposure to: (I) NaAc buffer, (II) NaAc buffer + H<sub>2</sub>O<sub>2</sub>, (III) PMCS, and (IV) PMCS + H<sub>2</sub>O<sub>2</sub>; the final working concentrations for NaAc buffer, H<sub>2</sub>O<sub>2</sub> and PMCS were 0.1 M, 100 μM, and 100 μg mL<sup>-1</sup>, respectively, (iii) photographs of *P. aeruginosa*-infected wound treated with (I)–(IV) at different days, (iv) histologic analysis of the wounds for (I)–(IV) after 6 days of therapy; scale bar is 500 μm. Reproduced with permission.<sup>158</sup> Copyright 2019, Wiley-VCH, (v) schematic of Fe SAzymes for antibiotics, (vi) schematic of the NIR-involved antibacterial experiment, (vii) IR images, (viii) digital photographs of the remaining bacteria-inoculated agar plates. Reproduced with permission.<sup>160</sup> Copyright 2019, Wiley-VCH. (h) and (i) Concept of using the nanozyme-based bandage with single-atom catalysis for the treatment of brain trauma. Reproduced with permission.<sup>157</sup> Copyright 2019, ACS, (ii) schematic of the formation of Co/PMCS, and (iii) their use as multi-antioxidant SAzymes for sepsis-management defeating nanozymes. Reproduced with permission.<sup>161</sup> Copyright 2019, Wiley-VCH.

(e.g. A $\beta$  plaques or tau tangles) without affecting normal biological processes. For instance, an SAC designed to degrade A $\beta$  should not interfere with other peptides or proteins<sup>144</sup> critical for normal brain function.<sup>145</sup>

## 6.2. Stability in biological systems

Atoms typically measure between 3 to 5 Å ( $10^{-10}$  m), while nanomaterials are sized around  $10^{-9}$  m. This size differential allows the attachment of multiple atoms to surfaces using nanomaterials as scaffolds. In catalytic processes, each atom acts as an operator, akin to an intricate production line. When applied in biological contexts, these catalytic targets are often proteins, and the transformation of nanomaterials into single-atom catalytic enzymes (SAzymes) illustrates the promising potential of single-atom nanozyme (SAN) technology for biological applications. Single atoms can be integrated into SAN materials, such as metal–organic frameworks<sup>146</sup> and carbon quantum dots (CQDs),<sup>147–150</sup> which serve as carriers and exhibit significantly higher reaction efficiencies than conventional enzymes. These carrier materials vary in size from 1 to 100 nm. Additionally, the optical properties of the support materials allow the nanocomposite to influence chemical reactions by absorbing radiation.<sup>151</sup> SAzymes, a novel class of high-performance nanozymes, have garnered significant research interest. Their homogeneously distributed active sites and unique coordination structures offer exceptional opportunities to explore the structure–activity relationship and fine-tune the geometric and electronic properties of catalytic active sites. SAzymes have made considerable progress in design synthesis, mechanistic understanding, and advanced applications. Their uniformly distributed catalytic active sites maximize atom efficiency, selectivity, and catalytic activity, making them particularly useful in maintaining structural integrity and function in the human brain's complex biochemical environment. This includes resistance to oxidation, proteolysis, and other degradation forms. For diagnostic and therapeutic uses, it is crucial that SACs and SAzymes remain stable in colloidal form to prevent aggregation or precipitation, which could otherwise lead to blockages in blood vessels or neural tissues.<sup>152</sup>

## 6.3. Biocompatibility and low toxicity

The design of SANs is crucially dependent on the biocompatibility of both the nanosupport, and the metal used. Transition metals, which are often employed due to their abundant d orbital domains, readily coordinate with nanosupport materials. The redox-active properties of these metals can disrupt redox homeostasis in tumour cells, making them suitable for therapeutic applications. Candidate metals can be fine-tuned to enhance the enzyme-like activity by optimizing their coordination structures with various nanosupport systems.<sup>153</sup> Unlike natural enzymes, SANs undergo a distinct catalytic process that involves substrate adsorption, surface reactions, and subsequent product dissociation, followed by the regeneration of active sites. Therefore, the surface structure of SANs plays a pivotal role in their catalytic efficiency. Surface modification is the most effective strategy for improving these properties,

allowing SANs to disperse effectively in biomimetic fluids. For instance, polyethylene glycol (PEG) is commonly used to enhance the hydrophilicity and biocompatibility of SANs.<sup>153</sup> PEG molecules reduce interactions with biological fluid components, thereby minimizing mononuclear phagocytosis clearance and prolonging the circulation time of SANs in the bloodstream. In addition to PEG, polyvinylpyrrolidone (PVP) is frequently used as a surface modifier to improve the dispersibility of SANs. These surface modifications further functionalize SANs, enhancing their bioaccumulation in both *in vivo* and *in vitro* settings. This functionalization equips SANs with capabilities that are advantageous for bacterial and cancer therapies, multimodal imaging, and tumour targeting.<sup>151</sup>

## 6.4. Redox activity for ROS regulation

Oxidative stress is a significant factor in the progression of AD. SACs and SAzymes play a crucial role in regulating reactive oxygen species (ROS) through redox reactions, mimicking the activities of enzymes like superoxide dismutase (SOD) and catalase (CAT). By controlling ROS levels, these nanozymes protect neurons from oxidative damage, potentially slowing AD progression.<sup>154</sup> In the accompanying Fig. 5, SAzymes are depicted demonstrating their redox activity for ROS regulation, mimicking enzyme activities, such as oxidase (OXD), peroxidase (POD), catalase (CAT), and superoxide dismutase (SOD).<sup>152</sup> Natural oxidases are enzymes that catalyze the oxidation of substrates, resulting in the production of oxidized products along with H<sub>2</sub>O, H<sub>2</sub>O<sub>2</sub>, or O<sub>2</sub>, particularly in the presence of molecular oxygen (O<sub>2</sub>) or other oxidants.

Recently, there have been reports of SAzymes, which are synthetic analogues, demonstrating oxidase-like (OXD-like) activity. For instance, Fe–N–C SAzymes, which feature atomically dispersed metal active sites, have shown remarkable OXD-like catalytic abilities.<sup>162</sup> These SAzymes can catalyze the conversion of O<sub>2</sub> into reactive oxygen species (ROS), such as superoxide radicals (O<sub>2</sub><sup>•−</sup>). Additionally, in the presence of O<sub>2</sub>, Fe–N–C SAzymes can oxidize 3,3',5,5'-tetramethylbenzidine (TMB), resulting in a blue-colored oxidized product (ox-TMB). Further studies have revealed that Fe–N–C SAzymes with Fe–N<sub>x</sub> active sites also exhibit OXD-like catalytic activity. These active sites are capable of reductively activating O<sub>2</sub> to produce various ROS, including superoxide radicals (O<sub>2</sub><sup>•−</sup>), hydrogen peroxide (H<sub>2</sub>O<sub>2</sub>), and singlet oxygen (<sup>1</sup>O<sub>2</sub>). Specifically, Fe–N<sub>3</sub> species within Fe–N/C–CNT SAzymes have been identified as the key OXD-mimicking active sites. The catalytic mechanism of these SAzymes likely involves the ROS generated during the O<sub>2</sub>-activation process, contributing to their OXD-mimicking activity. This discussion highlights the potential of SAzymes as synthetic alternatives to natural oxidases, offering insights into their catalytic mechanisms and applications.<sup>152</sup> Expanding material systems is still important, even though there are some findings on SAzymes that can scavenge ROS and reduce cellular oxidative damage. However, these reports are restricted to a few materials. Yet, significant work needs to be done in this area because the intrinsic mechanisms of ROS scavenging for SAzymes are currently unclear.

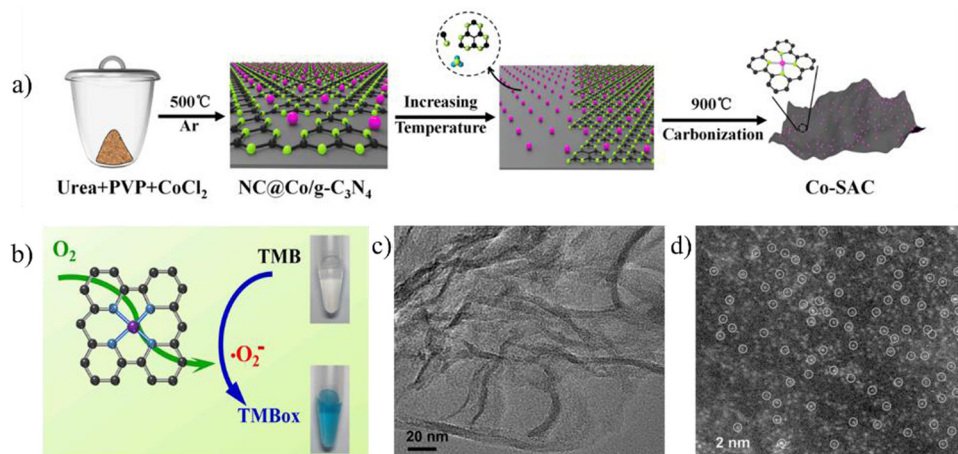


Fig. 6 (a) Synthesis of Co-SAC, (b) mechanism of the oxidase-like activity of Co-SAC, (c) and (d) TEM and AC-HAADF-STEM images. Reproduced with permission.<sup>136</sup> Copyright 2022, Elsevier.

## 7. SACs and SAzymes: a paradigm shift in catalysis towards biological systems

SACs have recently emerged as a revolutionary class of catalysts, demonstrating outstanding performance in terms of activity, stability, and selectivity across various significant chemical reactions. SACs combine the benefits of both homogeneous and heterogeneous catalysis, offering unparalleled efficiency in atom utilization, distinct quantum size effects, low coordination environments for individual atoms, and tuneable metal-support interactions, as depicted in Fig. 6. These unique characteristics make SACs highly promising for applications in renewable energy-conversion technologies and critical industrial processes. The geometric and electronic structures of SACs, intricately linked to their coordination and composition, play a crucial role in determining their catalytic effectiveness. Consequently, the controllable synthesis and rational design of SACs have become central focuses in the quest for cost-effective and environmentally friendly catalysis, with particular emphasis on optimizing atom economy.<sup>163,164</sup>

As heterogeneous catalysts, SAzymes are widely recognized for their robust stability, even under elevated temperatures and pressures, and for the ease with which they can be recovered from reactants and products. The coordination and electronic environment of metal-centred sites are pivotal in influencing the catalytic performance. However, conventional heterogeneous catalysts often suffer from inadequate atom utilization, as only a small fraction of the surface metal atoms actively engage in the reaction. This limitation has spurred the rapid development of advanced catalysts (SAzymes), representing a novel frontier in catalytic research, as depicted in Fig. 7. The presence of coordination-unsaturated surface atoms located at corners, edges, and steps, combined with the distinctive morphology of nanoparticles, plays a crucial role in modulating the adsorption and activation of reactant molecules, thereby enhancing the catalytic efficiency.<sup>165–168</sup>

## 8. Key advancements and obstacles in implementing SACs and SAzymes

SACs have emerged as a superior alternative to other 2D biomaterials, as they exhibit higher catalytic efficiency due to their fully exposed single metal atoms, enhanced selectivity, and increased sensitivity from their high surface area, enabling them to become a promising evolution in the early detection of diseases.<sup>169–171</sup> They also exhibit improved stability, are cost-effective and environmentally friendly due to reduced metal usage, and offer versatility in functionalisation. To further enhance their properties nanozymes have been incorporated in them (SAzymes), enabling a higher catalytic efficiency with nearly 100% atom utilization, superior selectivity through uniform active sites, and enhanced sensitivity. They are also more stable, cost-effective, and have lower toxicity. SAzymes have been designed to mimic natural enzymes, offering greater specificity for pathological conditions, better biocompatibility, and dynamic catalytic activity regulated by environmental factors.<sup>171–173</sup> Additionally, SAzymes allow for precise functionalization for biomarker targeting, tailored kinetics for metabolic processes, and greater structural diversity, making them more suitable for biomedical applications.<sup>174,175</sup> However, several critical challenges hinder their practical application, as outlined below.

### 8.1. Stability and selectivity

In the physiological conditions of the human system, the stability and selectivity of SAzymes and SACs is a major concern. These atomic materials are prone to forming metal-metal clusters over time, which can negatively impact their catalytic efficiency and reproducibility.<sup>176,177</sup> Also, while detecting reliable biomarkers for Alzheimer's APOE ε4 allele variation, cross-reactions with other biomolecules can lead to nonspecific binding and signal interference.

### 8.2. Reproducibility and scalability

The large-scale synthesis of SACs and SAzymes with consistent performance is difficult. The precise control and uniform

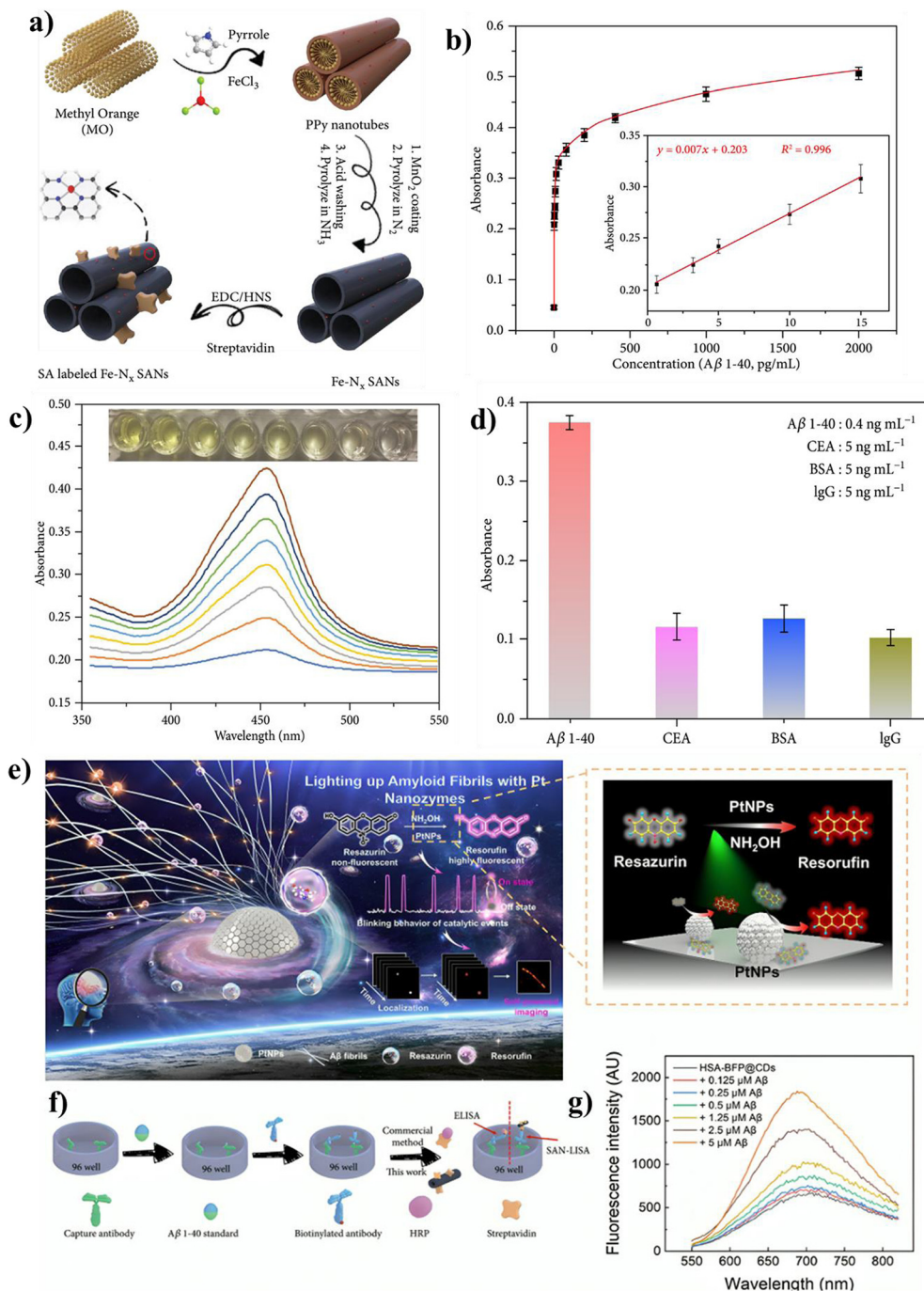


Fig. 7 (a) SA-labelled Fe-N<sub>x</sub> SANS, (b) and (c) sensitivity and absorbance graphs of different concentrations of Aβ 1-40, (d) selectivity of Fe-N<sub>x</sub> SANS towards Aβ 1-40. Reproduced with permission.<sup>44</sup> Copyright Science Partner Journals. (e) Pt nanozymes-catalyzed continuous formation of the fluorescent label RF for Aβ self-powered imaging of aggregates. Reproduced with permission.<sup>41</sup> Copyright 2023, Elsevier. (f) Test Aβ SAN-LISA schematic. (g) Fluorescence spectra of HSA-BFP and HSA-BFP@CDs reacting under different concentrations of Aβ. Reproduced with permission.<sup>40</sup> Copyright 2022, Elsevier.

dispersion of atomic metal atoms over the active sites in SAzymes require advanced and often expensive techniques. Scaling these synthesis methods for commercial production while maintaining the reproducibility and cost of the device is another major hurdle.

To overcome these challenges more advanced techniques, such as mass-selected soft-landing, atomic layer deposition (ALD), the solid-state diffusion method, and many others have

been explored to scale up the production with a higher metal loading capacity and uniform accumulation.<sup>178,179</sup> Further, SAzymes and SACs have been developed coordinated with carbon supports and metal-organic frameworks, whereby the precious metal catalysts are replaced with economical alternatives that exhibit remarkable catalytic efficiency and stability.<sup>68,69,180</sup> Derived from MOFs, SACs have demonstrated exceptional potential. This strategy holds great promise for

generating SACs characterized by an elevated metal loading and uniform distribution. However, this process results in the degradation of the carbon surface and the impairment of active catalytic sites. Second, it is difficult to stabilize isolated metal atoms on carbon supports without compromising their catalytic activities, particularly under elevated reaction environments.<sup>181,182</sup>

This challenge stems from the higher mobility of individual metal atoms, making them more prone to aggregation into larger particles due to their higher surface energies compared to corresponding metal clusters and nanoparticles (NPs). To effectively stabilize isolated metal atoms, the metal mass loading in current CS-SACs is intentionally kept low to minimize metal atom agglomeration. Third, owing to the diverse and complex structures, precise atom arrangements and identifying the origin of catalytic activity pose significant challenges. Consequently, diverse and well-thought-out rational design strategies are essential for the continued advancement of CS-SACs.<sup>176,183,184</sup>

## 9. Conclusion

This review precisely addressed the great potential of single-atom catalysts/nanozymes (SAzymes) as promising candidates for Alzheimer's disease early-stage detection. The therapeutic approach of SAC/SANs provides a unique crossroads for nanoscience and medicine. Since SANs can mimic the structure as well as the catalytic properties of natural enzymes they can exponentially increase the detection capability of SAzymes. The improved selectivity and sensitivity of SACs/SANs positions them as promising tools for targeting the complex mechanisms of cognitive diseases (like Alzheimer's disease). In this paper, we discussed how SANs bridge the gap between conventional enzymes and nanozymes, providing controlled electron transfer, good catalytic efficiency, and biosafety in the field of medicine. However, further research is needed to address the challenges and limitations associated with SACs and SAzymes to fully utilize their clinical applications. In summary, these barriers highlight the importance of further research attempting to address and overcome the limitations that prevent the widespread use of SACs in the clinical setting. As the work progresses, the redesign and translation of SACs/SANs into useful clinical applications may redefine Alzheimer's disease treatment in the future.

## Author contributions

HG: investigation, data curation, writing – original draft; IR: resources; KJ: visualization, KRR: project administration; VM: conceptualization, supervision, funding acquisition.

## Data availability

No primary research results, software or code have been included and no new data were generated or analyzed as part of this review.

## Conflicts of interest

There are no conflicts of interest to declare.

## Acknowledgements

The authors duly acknowledge the Science and Engineering Research Board, New Delhi for the financial support in the terms of the SERB-TARE Project (TAR/2022/000673), Amity Institute of Click Chemistry Research and Studies (AICCRS), and Amity University, Noida for providing the facilities.

## References

- 1 W. N. R. W. Isahak and A. Al-Amiery, Catalysts driving efficiency and innovation in thermal reactions: A comprehensive review, *Green Technol. Sustainability*, 2024, **2**, 100078, DOI: [10.1016/j.grets.2024.100078](https://doi.org/10.1016/j.grets.2024.100078).
- 2 V. Mishra, J. K. Cho, S.-H. Shin, Y.-W. Suh, H. S. Kim and Y.-J. Kim, Ruthenium-Na<sub>2</sub>CO<sub>3</sub> catalyzed one-pot synthesis of ring hydrogenated carbamates from aromatic amines and organic carbonates under H<sub>2</sub>, *Appl. Catal., A*, 2014, **487**, 82–90, DOI: [10.1016/j.apcata.2014.09.013](https://doi.org/10.1016/j.apcata.2014.09.013).
- 3 N. Yadav and V. Mishra, in *Catalytic Applications of Cerium-based Material, Cerium-Based Material: Synthesis, Properties, and Applications (Bentham Books)*, ISBN: 978-981-5080-09-4, 2023.
- 4 V. Mishra, S. Aggarwal and S. Pandey, in *Porous Polymer for Heterogeneous Catalysis, Porous Polymer Science and Applications*, CRC Press, 2022, pp. 91–120.
- 5 D. Mudgal, N. Yadav and V. Mishra, Nickel-doped magnetic carbon aerogel derived from xanthan gum: a competent catalyst for the degradation of single and binary dye-based water pollutants, *Environ. Sci. Pollut. Res.*, 2024, 1–13.
- 6 D. Mudgal, R. P. Singh, N. Yadav, T. Bharti and V. Mishra, Exploring the catalytic efficiency of copper-doped Magnetic Carbon Aerogel towards the coupling reaction of Isatin Oxime with Phenylboronic Acid derivatives, *SynOpen*, 2023, **7**(4), 570–579, DOI: [10.1055/a-2182-7757](https://doi.org/10.1055/a-2182-7757).
- 7 D. Mudgal, N. Yadav, J. Singh, G. K. Srivastava and V. Mishra, Xanthan gum-based copper nano-magnetite doped carbon aerogel: A promising candidate for environmentally friendly catalytic dye degradation, *Int. J. Biol. Macromol.*, 2023, **253**, 127491, DOI: [10.1016/j.ijbiomac.2023.127491](https://doi.org/10.1016/j.ijbiomac.2023.127491).
- 8 N. Yadav, R. P. Gaikwad, V. Mishra and M. B. Gawande, Synthesis and photocatalytic Applications of functionalized carbon quantum dots, *Bull. Chem. Soc. Jpn.*, 2022, **95**, 1638–1679.
- 9 X. Zheng, B. Li, Q. Wang, D. Wang and Y. Li, Emerging low-nuclearity supported metal catalysts with atomic level precision for efficient heterogeneous catalysis, *Nano Res.*, 2022, **15**, 7806–7839, DOI: [10.1007/s12274-022-4429-9](https://doi.org/10.1007/s12274-022-4429-9).
- 10 V. B. Saptal, V. Ruta, M. A. Bajada and G. Vilé, Single-Atom Catalysis in Organic Synthesis, *Angew. Chem., Int. Ed.*, 2023, **62**(34), e202219306, DOI: [10.1002/anie.202219306](https://doi.org/10.1002/anie.202219306).

- 11 R. Lang, X. Du, Y. Huang, X. Jiang, Q. Zhang, Y. Guo, K. Liu, B. Qiao, A. Wang and T. Zhang, Single-Atom Catalysts Based on the Metal–Oxide Interaction, *Chem. Rev.*, 2020, **120**, 11986–12043, DOI: [10.1021/acs.chemrev.0c00797](https://doi.org/10.1021/acs.chemrev.0c00797).
- 12 B. Chang, S. Wu, Y. Wang, T. Sun and Z. Cheng, Emerging single-atom iron catalysts for advanced catalytic systems, *Nanoscale Horiz.*, 2022, **7**, 1340–1387, DOI: [10.1039/D2NH00362G](https://doi.org/10.1039/D2NH00362G).
- 13 N. Cheng and X. Sun, Single atom catalyst by atomic layer deposition technique, *Chin. J. Catal.*, 2017, **38**, 1508–1514, DOI: [10.1016/S1872-2067\(17\)62903-6](https://doi.org/10.1016/S1872-2067(17)62903-6).
- 14 T. Zhang, A. G. Walsh, J. Yu and P. Zhang, Single-atom alloy catalysts: structural analysis, electronic properties and catalytic activities, *Chem. Soc. Rev.*, 2021, **50**, 569–588, DOI: [10.1039/D0CS00844C](https://doi.org/10.1039/D0CS00844C).
- 15 P. L. Gai and E. D. Boyes, *In situ* visualisation and analysis of dynamic single atom processes in heterogeneous catalysts, *J. Mater. Chem. A Mater.*, 2022, **10**, 5850–5862, DOI: [10.1039/D1TA08307D](https://doi.org/10.1039/D1TA08307D).
- 16 H. Jiang, Q. He, C. Wang, H. Liu, Y. Zhang, Y. Lin, X. Zheng, S. Chen, P. M. Ajayan and L. Song, Definitive Structural Identification toward Molecule-Type Sites within 1D and 2D Carbon-Based Catalysts, *Adv. Energy Mater.*, 2018, **8**(19), 1800436, DOI: [10.1002/aenm.201800436](https://doi.org/10.1002/aenm.201800436).
- 17 Q. Xue, Z. Zhang, B. K. Y. Ng, P. Zhao and B. T. W. Lo, Recent Advances in the Engineering of Single-Atom Catalysts Through Metal–Organic Frameworks, *Top. Curr. Chem.*, 2021, **379**, 11, DOI: [10.1007/s41061-021-00324-y](https://doi.org/10.1007/s41061-021-00324-y).
- 18 A. Li, M. Xu, D. Ma and W. Zhou, *Case Studies: Aberration Corrected High-Angle Annular Dark-Field (AC-HAADF) Microscopy*, 2023, pp. 449–457, DOI: [10.1007/978-3-031-07125-6\\_21](https://doi.org/10.1007/978-3-031-07125-6_21).
- 19 A. Alarawi, V. Ramalingam and J.-H. He, Recent advances in emerging single atom confined two-dimensional materials for water splitting applications, *Mater. Today Energy*, 2019, **11**, 1–23, DOI: [10.1016/j.mtener.2018.10.014](https://doi.org/10.1016/j.mtener.2018.10.014).
- 20 Z. Kou, W. Zang, P. Wang, X. Li and J. Wang, Single atom catalysts: a surface heterocompound perspective, *Nanoscale Horiz.*, 2020, **5**, 757–764, DOI: [10.1039/D0NH00088D](https://doi.org/10.1039/D0NH00088D).
- 21 S. Tajik, Z. Dourandish, F. Garkani Nejad, H. Beitollahi, A. A. Afshar, P. M. Jahani and A. Di Bartolomeo, Review—Single-Atom Catalysts as Promising Candidates for Electrochemical Applications, *J. Electrochem. Soc.*, 2022, **169**, 046504, DOI: [10.1149/1945-7111/ac62c3](https://doi.org/10.1149/1945-7111/ac62c3).
- 22 L. Li, X. Chang, X. Lin, Z. J. Zhao and J. Gong, Theoretical insights into single-atom catalysts, *Chem. Soc. Rev.*, 2020, **49**, 8156–8178, DOI: [10.1039/d0cs00795a](https://doi.org/10.1039/d0cs00795a).
- 23 J. Liu, B. R. Bunes, L. Zang and C. Wang, Supported single-atom catalysts: synthesis, characterization, properties, and applications, *Environ. Chem. Lett.*, 2018, **16**, 477–505, DOI: [10.1007/s10311-017-0679-2](https://doi.org/10.1007/s10311-017-0679-2).
- 24 M. B. Gawande, K. Ariga and Y. Yamauchi, Single-Atom Catalysts, *Small*, 2021, **17**(16), 2101584, DOI: [10.1002/smll.202101584](https://doi.org/10.1002/smll.202101584).
- 25 C. Rivera-Cárcamo and P. Serp, Single Atom Catalysts on Carbon-Based Materials, *ChemCatChem*, 2018, **10**, 5058–5091, DOI: [10.1002/cctc.201801174](https://doi.org/10.1002/cctc.201801174).
- 26 L. Huang, J. Chen, L. Gan, J. Wang and S. Dong, Single-atom nanozymes, *Sci. Adv.*, 2019, **5**, eaav5490.
- 27 R. Zhang, X. Yan and K. Fan, Nanozymes Inspired by Natural Enzymes, *Acc Mater. Res.*, 2021, **2**, 534–547, DOI: [10.1021/accountsmr.1c00074](https://doi.org/10.1021/accountsmr.1c00074).
- 28 L. Jiao, H. Yan, Y. Wu, W. Gu, C. Zhu, D. Du and Y. Lin, When nanozymes meet single-atom catalysis, *Angew. Chem.*, 2020, **132**, 2585–2596.
- 29 Z. Guo, J. Hong, N. Song and M. Liang, Single-Atom Nanozymes: From Precisely Engineering to Extensive Applications, *Acc Mater. Res.*, 2024, **5**, 347–357, DOI: [10.1021/accountsmr.3c00250](https://doi.org/10.1021/accountsmr.3c00250).
- 30 W. Wu, L. Huang, E. Wang and S. Dong, Atomic engineering of single-atom nanozymes for enzyme-like catalysis, *Chem. Sci.*, 2020, **11**, 9741–9756, DOI: [10.1039/D0SC03522J](https://doi.org/10.1039/D0SC03522J).
- 31 Z. Guo, J. Hong, N. Song and M. Liang, Single-Atom Nanozymes: From Precisely Engineering to Extensive Applications, *Acc Mater. Res.*, 2024, **5**, 347–357, DOI: [10.1021/accountsmr.3c00250](https://doi.org/10.1021/accountsmr.3c00250).
- 32 H. Song, M. Zhang and W. Tong, Single-Atom Nanozymes: Fabrication, Characterization, Surface Modification and Applications of ROS Scavenging and Antibacterial, *Molecules*, 2022, **27**, 5426, DOI: [10.3390/molecules27175426](https://doi.org/10.3390/molecules27175426).
- 33 T. Shi, Y. Cui, H. Yuan, R. Qi and Y. Yu, Burgeoning Single-Atom Nanozymes for Efficient Bacterial Elimination, *Nanomaterials*, 2023, **13**, 2760, DOI: [10.3390/nano13202760](https://doi.org/10.3390/nano13202760).
- 34 L. Jiao, H. Yan, Y. Wu, W. Gu, C. Zhu, D. Du and Y. Lin, When Nanozymes Meet Single-Atom Catalysis, *Angew. Chem., Int. Ed.*, 2020, **59**, 2565–2576, DOI: [10.1002/anie.201905645](https://doi.org/10.1002/anie.201905645).
- 35 B. Xu, H. Wang, W. Wang, L. Gao, S. Li, X. Pan, H. Wang, H. Yang, X. Meng, Q. Wu, L. Zheng, S. Chen, X. Shi, K. Fan, X. Yan and H. Liu, A Single-Atom Nanozyme for Wound Disinfection Applications, *Angew. Chem., Int. Ed.*, 2019, **58**, 4911–4916, DOI: [10.1002/anie.201813994](https://doi.org/10.1002/anie.201813994).
- 36 J. Jia, Y. Ning, M. Chen, S. Wang, H. Yang, F. Li, J. Ding, Y. Li, B. Zhao, J. Lyu, S. Yang, X. Yan, Y. Wang, W. Qin, Q. Wang, Y. Li, J. Zhang, F. Liang, Z. Liao and S. Wang, Biomarker Changes during 20 Years Preceding Alzheimer's Disease, *N. Engl. J. Med.*, 2024, **390**, 712–722, DOI: [10.1056/NEJMoa2310168](https://doi.org/10.1056/NEJMoa2310168).
- 37 M. Askenazi, T. Kavanagh, G. Pires, B. Ueberheide, T. Wisniewski and E. Drummond, Compilation of reported protein changes in the brain in Alzheimer's disease, *Nat. Commun.*, 2023, **14**, 4466, DOI: [10.1038/s41467-023-40208-x](https://doi.org/10.1038/s41467-023-40208-x).
- 38 N. Yadav, D. Mudgal, S. Mishra, H. Sehwat, N. K. Singh, K. Sharma, P. C. Sharma, J. Singh and V. Mishra, Development of ionic liquid-capped carbon dots derived from Tecoma stans (L.) Juss. ex Kunth: Combatting bacterial pathogens in diabetic foot ulcer pus swabs, targeting both standard and multi-drug resistant strains, *S. Afr. J. Bot.*, 2023, **163**, 412–436, DOI: [10.1016/j.sajb.2023.10.063](https://doi.org/10.1016/j.sajb.2023.10.063).
- 39 X.-H. Wen, X.-F. Zhao, X.-H. Wang, Y. Wang, J.-C. Guo, H.-G. Zhou, C.-T. Zuo and H.-L. Lu, Fe<sub>3</sub>O<sub>4</sub>/MXene Nanosphere-Based Microfluidic Chip for the Accurate Diagnosis of Alzheimer's Disease, *ACS Appl. Nano Mater.*, 2022, **5**, 15925–15933, DOI: [10.1021/acsanm.2c04187](https://doi.org/10.1021/acsanm.2c04187).

- 40 W. Wang, X. Lin, X. Dong and Y. Sun, A multi-target theranostic nano-composite against Alzheimer's disease fabricated by conjugating carbon dots and triple-functionalized human serum albumin, *Acta Biomater.*, 2022, **148**, 298–309, DOI: [10.1016/j.actbio.2022.06.029](https://doi.org/10.1016/j.actbio.2022.06.029).
- 41 X. Wang, Y. Li, L. Wei and L. Xiao, Direct visualization of  $\beta$ -amyloid fibrils with a self-powered imaging strategy through the generation of fluorescent tags with Pt nanozymes, *Chem. Eng. J.*, 2023, **471**, 144513, DOI: [10.1016/j.cej.2023.144513](https://doi.org/10.1016/j.cej.2023.144513).
- 42 S. Ding, J. A. Barr, Z. Lyu, F. Zhang, M. Wang, P. Tieu, X. Li, M. H. Engelhard, Z. Feng, S. P. Beckman, X. Pan, J. Li, D. Du and Y. Lin, Effect of Phosphorus Modulation in Iron Single-Atom Catalysts for Peroxidase Mimicking, *Adv. Mater.*, 2024, **36**(10), 2209633, DOI: [10.1002/adma.202209633](https://doi.org/10.1002/adma.202209633).
- 43 B. Li, Y. Bai, C. Yion, H. Wang, X. Su, G. Feng, M. Guo, W. Peng, B. Shen and B. Zheng, Single-Atom Nanocatalytic Therapy for Suppression of Neuroinflammation by Inducing Autophagy of Abnormal Mitochondria, *ACS Nano*, 2023, **17**, 7511–7529, DOI: [10.1021/acsnano.2c12614](https://doi.org/10.1021/acsnano.2c12614).
- 44 Z. Lyu, S. Ding, N. Zhang, Y. Zhou, N. Cheng, M. Wang, M. Xu, Z. Feng, X. Niu, Y. Cheng, C. Zhang, D. Du and Y. Lin, Single-Atom Nanozymes Linked Immunosorbent Assay for Sensitive Detection of A  $\beta$  1-40: A Biomarker of Alzheimer's Disease, *Research*, 2020, **2020**, 4724505, DOI: [10.34133/2020/4724505](https://doi.org/10.34133/2020/4724505).
- 45 Y.-W. Mao, J. Zhang, R. Zhang, J.-Q. Li, A.-J. Wang, X.-C. Zhou and J.-J. Feng, N-Doped Carbon Nanotubes Supported Fe–Mn Dual-Single-Atoms Nanozyme with Synergistically Enhanced Peroxidase Activity for Sensitive Colorimetric Detection of Acetylcholinesterase and Its Inhibitor, *Anal. Chem.*, 2023, **95**, 8640–8648, DOI: [10.1021/acs.analchem.3c01070](https://doi.org/10.1021/acs.analchem.3c01070).
- 46 J. Guan, M. Wang, R. Ma, Q. Liu, X. Sun, Y. Xiong and X. Chen, Single-atom Rh nanozyme: An efficient catalyst for highly sensitive colorimetric detection of acetylcholinesterase activity and adrenaline, *Sens. Actuators, B*, 2023, **375**, 132972, DOI: [10.1016/j.snb.2022.132972](https://doi.org/10.1016/j.snb.2022.132972).
- 47 N. Gong, X. Ma, X. Ye, Q. Zhou, X. Chen, X. Tan, S. Yao, S. Huo, T. Zhang, S. Chen, X. Teng, X. Hu, J. Yu, Y. Gan, H. Jiang, J. Li and X.-J. Liang, Carbon-dot-supported atomically dispersed gold as a mitochondrial oxidative stress amplifier for cancer treatment, *Nat. Nanotechnol.*, 2019, **14**, 379–387, DOI: [10.1038/s41565-019-0373-6](https://doi.org/10.1038/s41565-019-0373-6).
- 48 J. Wu, Y. Wu, L. Lu, D. Zhang and X. Wang, Single-atom Au catalyst loaded on CeO<sub>2</sub>: A novel single-atom nanozyme electrochemical H<sub>2</sub>O<sub>2</sub> sensor, *Talanta Open*, 2021, **4**, 100075, DOI: [10.1016/j.talo.2021.100075](https://doi.org/10.1016/j.talo.2021.100075).
- 49 Q. Chen, M. Zhang, H. Huang, C. Dong, X. Dai, G. Feng, L. Lin, D. Sun, D. Yang, L. Xie, Y. Chen, J. Guo and X. Jing, Single Atom-Doped Nanosensitizers for Mutually Optimized Sono/Chemo-Nanodynamic Therapy of Triple Negative Breast Cancer, *Adv. Sci.*, 2023, **10**(6), 2206244, DOI: [10.1002/advs.202206244](https://doi.org/10.1002/advs.202206244).
- 50 S. Cai, J. Liu, J. Ding, Z. Fu, H. Li, Y. Xiong, Z. Lian, R. Yang and C. Chen, Tumor-Microenvironment-Responsive Cascade Reactions by a Cobalt-Single-Atom Nanozyme for Synergistic Nanocatalytic Chemotherapy, *Angew. Chem., Int. Ed.*, 2022, **134**(48), e202204502, DOI: [10.1002/anie.202204502](https://doi.org/10.1002/anie.202204502).
- 51 B. Xu, S. Li, L. Zheng, Y. Liu, A. Han, J. Zhang, Z. Huang, H. Xie, K. Fan, L. Gao and H. Liu, A Bioinspired Five-Coordinated Single-Atom Iron Nanozyme for Tumor Catalytic Therapy, *Adv. Mater.*, 2022, **34**(15), 2107088, DOI: [10.1002/adma.202107088](https://doi.org/10.1002/adma.202107088).
- 52 Y. Zhu, W. Wang, P. Gong, Y. Zhao, Y. Pan, J. Zou, R. Ao, J. Wang, H. Cai, H. Huang, M. Yu, H. Wang, L. Lin, X. Chen and Y. Wu, Enhancing Catalytic Activity of a Nickel Single Atom Enzyme by Polynary Heteroatom Doping for Ferroptosis-Based Tumor Therapy, *ACS Nano*, 2023, **17**, 3064–3076, DOI: [10.1021/acsnano.2c11923](https://doi.org/10.1021/acsnano.2c11923).
- 53 Y. Chen, H. Zou, B. Yan, X. Wu, W. Cao, Y. Qian, L. Zheng and G. Yang, Atomically Dispersed Cu Nanozyme with Intensive Ascorbate Peroxidase Mimic Activity Capable of Alleviating ROS-Mediated Oxidation Damage, *Adv. Sci.*, 2022, **9**(5), 2103977, DOI: [10.1002/advs.202103977](https://doi.org/10.1002/advs.202103977).
- 54 X. Wang, Q. Chen, Y. Zhu, K. Wang, Y. Chang, X. Wu, W. Bao, T. Cao, H. Chen, Y. Zhang and H. Qin, Destroying pathogen-tumor symbionts synergizing with catalytic therapy of colorectal cancer by biomimetic protein-supported single-atom nanozyme, *Signal Transduction Targeted Ther.*, 2023, **8**, 277, DOI: [10.1038/s41392-023-01491-8](https://doi.org/10.1038/s41392-023-01491-8).
- 55 D. Yang, H. Yu, T. He, S. Zuo, X. Liu, H. Yang, B. Ni, H. Li, L. Gu, D. Wang and X. Wang, Visible-light-switched electron transfer over single porphyrin-metal atom center for highly selective electroreduction of carbon dioxide, *Nat. Commun.*, 2019, **10**, 3844, DOI: [10.1038/s41467-019-11817-2](https://doi.org/10.1038/s41467-019-11817-2).
- 56 D. Wang and Y. Zhao, Single-atom engineering of metal-organic frameworks toward healthcare, *Chem*, 2021, **7**, 2635–2671, DOI: [10.1016/j.chempr.2021.08.020](https://doi.org/10.1016/j.chempr.2021.08.020).
- 57 M. Chang, Z. Hou, M. Wang, C. Yang, R. Wang, F. Li, D. Liu, T. Peng, C. Li and J. Lin, Single-Atom Pd Nanozyme for Ferroptosis-Boosted Mild-Temperature Photothermal Therapy, *Angew. Chem., Int. Ed.*, 2021, **60**, 12971–12979, DOI: [10.1002/anie.202101924](https://doi.org/10.1002/anie.202101924).
- 58 S. Fu, C. Zhu, D. Su, J. Song, S. Yao, S. Feng, M. H. Engelhard, D. Du and Y. Lin, Porous Carbon-Hosted Atomically Dispersed Iron–Nitrogen Moiety as Enhanced Electrocatalysts for Oxygen Reduction Reaction in a Wide Range of pH, *Small*, 2018, **14**(12), 1703118, DOI: [10.1002/smll.201703118](https://doi.org/10.1002/smll.201703118).
- 59 B. Xu, H. Wang, W. Wang, L. Gao, S. Li, X. Pan, H. Wang, H. Yang, X. Meng, Q. Wu, L. Zheng, S. Chen, X. Shi, K. Fan, X. Yan and H. Liu, A Single-Atom Nanozyme for Wound Disinfection Applications, *Angew. Chem.*, 2019, **131**, 4965–4970, DOI: [10.1002/ange.201813994](https://doi.org/10.1002/ange.201813994).
- 60 J. Zhu, Q. Li, X. Li, X. Wu, T. Yuan and Y. Yang, Simulated Enzyme Activity and Efficient Antibacterial Activity of Copper-Doped Single-Atom Nanozymes, *Langmuir*, 2022, **38**, 6860–6870, DOI: [10.1021/acs.langmuir.2c00155](https://doi.org/10.1021/acs.langmuir.2c00155).
- 61 Y. Feng, J. Qin, Y. Zhou, Q. Yue and J. Wei, Spherical mesoporous Fe–N–C single-atom nanozyme for

- photothermal and catalytic synergistic antibacterial therapy, *J. Colloid Interface Sci.*, 2022, **606**, 826–836, DOI: [10.1016/j.jcis.2021.08.054](https://doi.org/10.1016/j.jcis.2021.08.054).
- 62 Q. Hong, H. Yang, Y. Fang, W. Li, C. Zhu, Z. Wang, S. Liang, X. Cao, Z. Zhou, Y. Shen, S. Liu and Y. Zhang, Adaptable graphitic C<sub>6</sub>N<sub>6</sub>-based copper single-atom catalyst for intelligent biosensing, *Nat. Commun.*, 2023, **14**, 2780, DOI: [10.1038/s41467-023-38459-9](https://doi.org/10.1038/s41467-023-38459-9).
- 63 H. He, Z. Fei, T. Guo, Y. Hou, D. Li, K. Wang, F. Ren, K. Fan, D. Zhou, C. Xie, C. Wang and X. Lu, Bioadhesive injectable hydrogel with phenolic carbon quantum dot supported Pd single atom nanozymes as a localized immunomodulation niche for cancer catalytic immunotherapy, *Biomaterials*, 2022, **280**, 121272, DOI: [10.1016/j.biomaterials.2021.121272](https://doi.org/10.1016/j.biomaterials.2021.121272).
- 64 Y. Zhu, W. Wang, J. Cheng, Y. Qu, Y. Dai, M. Liu, J. Yu, C. Wang, H. Wang, S. Wang, C. Zhao, Y. Wu and Y. Liu, Stimuli-Responsive Manganese Single-Atom Nanozyme for Tumor Therapy via Integrated Cascade Reactions, *Angew. Chem.*, 2021, **133**, 9566–9574, DOI: [10.1002/ange.202017152](https://doi.org/10.1002/ange.202017152).
- 65 D. Wang, H. Wu, S. Z. F. Phua, G. Yang, W. Qi Lim, L. Gu, C. Qian, H. Wang, Z. Guo, H. Chen and Y. Zhao, Self-assembled single-atom nanozyme for enhanced photodynamic therapy treatment of tumor, *Nat. Commun.*, 2020, **11**, 357, DOI: [10.1038/s41467-019-14199-7](https://doi.org/10.1038/s41467-019-14199-7).
- 66 Y. Fan, X. Gan, H. Zhao, Z. Zeng, W. You and X. Quan, Multiple application of SAzyme based on carbon nitride nanorod-supported Pt single-atom for H<sub>2</sub>O<sub>2</sub> detection, antibiotic detection and antibacterial therapy, *Chem. Eng. J.*, 2022, **427**, 131572, DOI: [10.1016/j.cej.2021.131572](https://doi.org/10.1016/j.cej.2021.131572).
- 67 S. Ji, B. Jiang, H. Hao, Y. Chen, J. Dong, Y. Mao, Z. Zhang, R. Gao, W. Chen, R. Zhang, Q. Liang, H. Li, S. Liu, Y. Wang, Q. Zhang, L. Gu, D. Duan, M. Liang, D. Wang, X. Yan and Y. Li, Matching the kinetics of natural enzymes with a single-atom iron nanozyme, *Nat. Catal.*, 2021, **4**, 407–417, DOI: [10.1038/s41929-021-00609-x](https://doi.org/10.1038/s41929-021-00609-x).
- 68 W. Guo, Z. Wang, X. Wang and Y. Wu, General Design Concept for Single-Atom Catalysts toward Heterogeneous Catalysis, *Adv. Mater.*, 2021, **33**, 2004287, DOI: [10.1002/adma.202004287](https://doi.org/10.1002/adma.202004287).
- 69 L. Hu, W. Li, L. Wang and B. Wang, Turning metal-organic frameworks into efficient single-atom catalysts via pyrolysis with a focus on oxygen reduction reaction catalysts, *Energy Chem.*, 2021, **3**, 100056, DOI: [10.1016/j.enchem.2021.100056](https://doi.org/10.1016/j.enchem.2021.100056).
- 70 H. Zhou, S. Hong, H. Zhang, Y. Chen, H. Xu, X. Wang, Z. Jiang, S. Chen and Y. Liu, Toward biomass-based single-atom catalysts and plastics: Highly active single-atom Co on N-doped carbon for oxidative esterification of primary alcohols, *Appl. Catal., B*, 2019, **256**, 117767, DOI: [10.1016/j.apcatb.2019.117767](https://doi.org/10.1016/j.apcatb.2019.117767).
- 71 J.-C. Liu, H. Xiao and J. Li, Constructing High-Loading Single-Atom/Cluster Catalysts via an Electrochemical Potential Window Strategy, *J. Am. Chem. Soc.*, 2020, **142**, 3375–3383, DOI: [10.1021/jacs.9b06808](https://doi.org/10.1021/jacs.9b06808).
- 72 H. Xiang, W. Feng and Y. Chen, Single-Atom Catalysts in Catalytic Biomedicine, *Adv. Mater.*, 2020, **32**, 1905994, DOI: [10.1002/adma.201905994](https://doi.org/10.1002/adma.201905994).
- 73 X. Wang, B. Jin, Y. Jin, T. Wu, L. Ma and X. Liang, Supported Single Fe Atoms Prepared via Atomic Layer Deposition for Catalytic Reactions, *ACS Appl. Nano Mater.*, 2020, **3**, 2867–2874, DOI: [10.1021/acsanm.0c00146](https://doi.org/10.1021/acsanm.0c00146).
- 74 L. Cao and J. Lu, Atomic-scale engineering of metal–oxide interfaces for advanced catalysis using atomic layer deposition, *Catal. Sci. Technol.*, 2020, **10**, 2695–2710, DOI: [10.1039/DOCY00304B](https://doi.org/10.1039/DOCY00304B).
- 75 J.-C. Liu, H. Xiao and J. Li, Constructing High-Loading Single-Atom/Cluster Catalysts via an Electrochemical Potential Window Strategy, *J. Am. Chem. Soc.*, 2020, **142**, 3375–3383, DOI: [10.1021/jacs.9b06808](https://doi.org/10.1021/jacs.9b06808).
- 76 Y. Chen, Z. Ma and X. Tang, in *Single-Atom Heterogeneous Catalysts*, *Heterogeneous Catalysts*, Wiley, 2021, pp. 103–117, DOI: [10.1002/9783527813599.ch6](https://doi.org/10.1002/9783527813599.ch6).
- 77 S. Zhao, G. Chen, G. Zhou, L. Yin, J. Veder, B. Johannessen, M. Saunders, S. Yang, R. De Marco, C. Liu and S. P. Jiang, A Universal Seeding Strategy to Synthesize Single Atom Catalysts on 2D Materials for Electrocatalytic Applications, *Adv. Funct. Mater.*, 2020, **30**, 1906157, DOI: [10.1002/adfm.201906157](https://doi.org/10.1002/adfm.201906157).
- 78 L. Zhang, X. Zhao, Z. Yuan, M. Wu and H. Zhou, Oxygen defect-stabilized heterogeneous single atom catalysts: preparation, properties and catalytic application, *J. Mater. Chem. A*, 2021, **9**, 3855–3879, DOI: [10.1039/D0TA10541D](https://doi.org/10.1039/D0TA10541D).
- 79 L. Hu, W. Li, L. Wang and B. Wang, Turning metal-organic frameworks into efficient single-atom catalysts via pyrolysis with a focus on oxygen reduction reaction catalysts, *Energy-Chem*, 2021, **3**, 100056, DOI: [10.1016/j.enchem.2021.100056](https://doi.org/10.1016/j.enchem.2021.100056).
- 80 J. Li, C. Chen, L. Xu, Y. Zhang, W. Wei, E. Zhao, Y. Wu and C. Chen, Challenges and Perspectives of Single-Atom-Based Catalysts for Electrochemical Reactions, *JACS Au*, 2023, **3**, 736–755, DOI: [10.1021/jacsau.3c00001](https://doi.org/10.1021/jacsau.3c00001).
- 81 J. Wu, H. Shi, K. Li and X. Guo, Advances and challenges of single-atom catalysts in environmental catalysis, *Curr. Opin. Chem. Eng.*, 2023, **40**, 100923, DOI: [10.1016/j.coche.2023.100923](https://doi.org/10.1016/j.coche.2023.100923).
- 82 X. He, Y. Deng, Y. Zhang, Q. He, D. Xiao, M. Peng, Y. Zhao, H. Zhang, R. Luo, T. Gan, H. Ji and D. Ma, Mechanochemical Kilogram-Scale Synthesis of Noble Metal Single-Atom Catalysts, *Cell Rep. Phys. Sci.*, 2020, **1**, 100004, DOI: [10.1016/j.xcrp.2019.100004](https://doi.org/10.1016/j.xcrp.2019.100004).
- 83 M. Flytzani-Stephanopoulos and B. C. Gates, Atomically Dispersed Supported Metal Catalysts, *Annu. Rev. Chem. Biomol. Eng.*, 2012, **3**, 545–574, DOI: [10.1146/annurev-chembioeng-062011-080939](https://doi.org/10.1146/annurev-chembioeng-062011-080939).
- 84 V. Muravev, G. Spezzati, Y.-Q. Su, A. Parastaev, F.-K. Chiang, A. Longo, C. Escudero, N. Kosinov and E. J. M. Hensen, Interface dynamics of Pd–CeO<sub>2</sub> single-atom catalysts during CO oxidation, *Nat. Catal.*, 2021, **4**, 469–478, DOI: [10.1038/s41929-021-00621-1](https://doi.org/10.1038/s41929-021-00621-1).
- 85 J. Wang, Z. Li, Y. Wu and Y. Li, Fabrication of Single-Atom Catalysts with Precise Structure and High Metal Loading, *Adv. Mater.*, 2018, **30**(48), 1801649, DOI: [10.1002/adma.201801649](https://doi.org/10.1002/adma.201801649).
- 86 L. Jiao and H.-L. Jiang, Metal-Organic-Framework-Based Single-Atom Catalysts for Energy Applications, *Chem*, 2019, **5**, 786–804, DOI: [10.1016/j.chempr.2018.12.011](https://doi.org/10.1016/j.chempr.2018.12.011).

- 87 Z.-Y. Wu, P. Zhu, D. A. Cullen, Y. Hu, Q.-Q. Yan, S.-C. Shen, F.-Y. Chen, H. Yu, M. Shakouri and J. D. Arregui-Mena, A general synthesis of single atom catalysts with controllable atomic and mesoporous structures, *Nat. Synthesis*, 2022, 658–667.
- 88 F. Manea, F. B. Houillon, L. Pasquato and P. Scrimin, Nanozymes: Gold-Nanoparticle-Based Transphosphorylation Catalysts, *Angew. Chem., Int. Ed.*, 2004, **43**, 6165–6169, DOI: [10.1002/anie.200460649](https://doi.org/10.1002/anie.200460649).
- 89 D. Wang, B. Zhang, H. Ding, D. Liu, J. Xiang, X. J. Gao, X. Chen, Z. Li, L. Yang, H. Duan, J. Zheng, Z. Liu, B. Jiang, Y. Liu, N. Xie, H. Zhang, X. Yan, K. Fan and G. Nie, TiO<sub>2</sub> supported single Ag atoms nanozyme for elimination of SARS-CoV2, *Nano Today*, 2021, **40**, 101243, DOI: [10.1016/j.nantod.2021.101243](https://doi.org/10.1016/j.nantod.2021.101243).
- 90 X. Yang, J. Xiang, W. Su, J. Guo, J. Deng, L. Tang, G. Li, Y. Liang, L. Zheng, M. He, J. Zhong and J. Zhao, Modulating Pt nanozyme by using isolated cobalt atoms to enhance catalytic activity for alleviating osteoarthritis, *Nano Today*, 2023, **49**, 101809, DOI: [10.1016/j.nantod.2023.101809](https://doi.org/10.1016/j.nantod.2023.101809).
- 91 G. Kyriakou, S. K. Beaumont and R. M. Lambert, Aspects of Heterogeneous Enantioselective Catalysis by Metals, *Langmuir*, 2011, **27**, 9687–9695, DOI: [10.1021/la200009w](https://doi.org/10.1021/la200009w).
- 92 B. Qiao, A. Wang, X. Yang, L. F. Allard, Z. Jiang, Y. Cui, J. Liu, J. Li and T. Zhang, Single-atom catalysis of CO oxidation using Pt1/FeO<sub>x</sub>, *Nat. Chem.*, 2011, **3**, 634–641, DOI: [10.1038/nchem.1095](https://doi.org/10.1038/nchem.1095).
- 93 X. Zhang, H. Shi and B. Xu, Catalysis by Gold: Isolated Surface Au<sup>3+</sup> Ions are Active Sites for Selective Hydrogenation of 1,3-Butadiene over Au/ZrO<sub>2</sub> Catalysts, *Angew. Chem., Int. Ed.*, 2005, **44**, 7132–7135, DOI: [10.1002/anie.200502101](https://doi.org/10.1002/anie.200502101).
- 94 Q. Fu, H. Saltsburg and M. Flytzani-Stephanopoulos, Active Nonmetallic Au and Pt Species on Ceria-Based Water-Gas Shift Catalysts, *Science*, 1979, **301**(2003), 935–938, DOI: [10.1126/science.1085721](https://doi.org/10.1126/science.1085721).
- 95 K. Yamaguchi, K. Mori, T. Mizugaki, K. Ebitani and K. Kaneda, Creation of a Monomeric Ru Species on the Surface of Hydroxyapatite as an Efficient Heterogeneous Catalyst for Aerobic Alcohol Oxidation, *J. Am. Chem. Soc.*, 2000, **122**, 7144–7145, DOI: [10.1021/ja001325i](https://doi.org/10.1021/ja001325i).
- 96 L. Fan, P. F. Liu, X. Yan, L. Gu, Z. Z. Yang, H. G. Yang, S. Qiu and X. Yao, Atomically isolated nickel species anchored on graphitized carbon for efficient hydrogen evolution electrocatalysis, *Nat. Commun.*, 2016, **7**, 10667.
- 97 C.-C. Hou, H.-F. Wang, C. Li and Q. Xu, From metal-organic frameworks to single/dual-atom and cluster metal catalysts for energy applications, *Energy Environ. Sci.*, 2020, **13**, 1658–1693.
- 98 Y. Wang, J. Mao, X. Meng, L. Yu, D. Deng and X. Bao, Catalysis with two-dimensional materials confining single atoms: concept, design, and applications, *Chem. Rev.*, 2018, **119**, 1806–1854.
- 99 J. Li, M. Chen, D. A. Cullen, S. Hwang, M. Wang, B. Li, K. Liu, S. Karakalos, M. Lucero and H. Zhang, Atomically dispersed manganese catalysts for oxygen reduction in proton-exchange membrane fuel cells, *Nat. Catal.*, 2018, **1**, 935–945.
- 100 Y. Chen, J. Lin, B. Jia, X. Wang, S. Jiang and T. Ma, Isolating single and few atoms for enhanced catalysis, *Adv. Mater.*, 2022, **34**, 2201796.
- 101 D. Bokov, A. Turki Jalil, S. Chupradit, W. Suksatan, M. Javed Ansari, I. H. Shewael, G. H. Valiev and E. Kianfar, Nanomaterial by sol-gel method: synthesis and application, *Adv. Mater. Sci. Eng.*, 2021, **2021**, 1–21.
- 102 J. Jones, H. Xiong, A. T. DeLaRiva, E. J. Peterson, H. Pham, S. R. Challa, G. Qi, S. Oh, M. H. Wiebenga and X. I. Pereira Hernández, Thermally stable single-atom platinum-on-ceria catalysts via atom trapping, *Science*, 1979, **353**(2016), 150–154.
- 103 L. Cao, W. Liu, Q. Luo, R. Yin, B. Wang, J. Weissenrieder, M. Soldemo, H. Yan, Y. Lin and Z. Sun, Atomically dispersed iron hydroxide anchored on Pt for preferential oxidation of CO in H<sub>2</sub>, *Nature*, 2019, **565**, 631–635.
- 104 M. Zhang, Y.-G. Wang, W. Chen, J. Dong, L. Zheng, J. Luo, J. Wan, S. Tian, W.-C. Cheong and D. Wang, Metal (hydr) oxides@ polymer core-shell strategy to metal single-atom materials, *J. Am. Chem. Soc.*, 2017, **139**, 10976–10979.
- 105 P. Liu, Y. Zhao, R. Qin, S. Mo, G. Chen, L. Gu, D. M. Chevrier, P. Zhang, Q. Guo and D. Zang, Photochemical route for synthesizing atomically dispersed palladium catalysts, *Science*, 1979, **352**(2016), 797–800.
- 106 M. Yang, L. F. Allard and M. Flytzani-Stephanopoulos, Atomically dispersed Au-(OH)<sub>x</sub> species bound on titania catalyze the low-temperature water-gas shift reaction, *J. Am. Chem. Soc.*, 2013, **135**, 3768–3771.
- 107 H. Wei, K. Huang, D. Wang, R. Zhang, B. Ge, J. Ma, B. Wen, S. Zhang, Q. Li and M. Lei, Iced photochemical reduction to synthesize atomically dispersed metals by suppressing nanocrystal growth, *Nat. Commun.*, 2017, **8**, 1490.
- 108 A. K. Datye and H. Guo, Single atom catalysis poised to transition from an academic curiosity to an industrially relevant technology, *Nat. Commun.*, 2021, **12**, 895, DOI: [10.1038/s41467-021-21152-0](https://doi.org/10.1038/s41467-021-21152-0).
- 109 T. Shimbayashi and K. Fujita, Recent Advances in Homogeneous Catalysis via Metal-Ligand Cooperation Involving Aromatization and Dearomatization, *Catalysts*, 2020, **10**, 635, DOI: [10.3390/catal10060635](https://doi.org/10.3390/catal10060635).
- 110 S. F. Yuk, G. Collinge, M.-T. Nguyen, M.-S. Lee, V.-A. Glezakou and R. Rousseau, *Single-Atom Catalysis: An Analogy between Heterogeneous and Homogeneous Catalysts*, 2020, pp. 1–15, DOI: [10.1021/bk-2020-1360.ch001](https://doi.org/10.1021/bk-2020-1360.ch001).
- 111 Y. Hu, G. Luo, L. Wang, X. Liu, Y. Qu, Y. Zhou, F. Zhou, Z. Li, Y. Li, T. Yao, C. Xiong, B. Yang, Z. Yu and Y. Wu, Single Ru Atoms Stabilized by Hybrid Amorphous/Crystalline FeCoNi Layered Double Hydroxide for Ultraefficient Oxygen Evolution, *Adv. Energy Mater.*, 2021, **11**(1), 2002816, DOI: [10.1002/aenm.202002816](https://doi.org/10.1002/aenm.202002816).
- 112 H. Lan, J. Wang, L. Cheng, D. Yu, H. Wang and L. Guo, The synthesis and application of crystalline-amorphous hybrid materials, *Chem. Soc. Rev.*, 2024, **53**, 684–713, DOI: [10.1039/D3CS00860F](https://doi.org/10.1039/D3CS00860F).
- 113 Z. Jiang, X. Feng, J. Deng, C. He, M. Douthwaite, Y. Yu, J. Liu, Z. Hao and Z. Zhao, Atomic-Scale Insights into the

- Low-Temperature Oxidation of Methanol over a Single-Atom Pt<sub>1</sub>-Co<sub>3</sub>O<sub>4</sub> Catalyst, *Adv. Funct. Mater.*, 2019, **29**(31), 1902041, DOI: [10.1002/adfm.201902041](https://doi.org/10.1002/adfm.201902041).
- 114 I. C. Neel, in *Alzheimer's Disease and Other Dementias, Geriatric Medicine*, Springer International Publishing, Cham, 2024, pp. 1027–1046, DOI: [10.1007/978-3-030-74720-6\\_84](https://doi.org/10.1007/978-3-030-74720-6_84).
- 115 M. R. Chorawala, A. C. Shah, A. J. Pandya, N. R. Kothari and B. G. Prajapati, in *Symptoms and conventional treatments of Alzheimer's disease, Alzheimer's Disease and Advanced Drug Delivery Strategies*, Elsevier, 2024, pp. 213–234, DOI: [10.1016/B978-0-443-13205-6.00009-1](https://doi.org/10.1016/B978-0-443-13205-6.00009-1).
- 116 A. R. Kamer, R. G. Craig, R. Niederman, J. Fortea and M. J. de Leon, Periodontal disease as a possible cause for Alzheimer's disease, *Periodontol*, 2020, (83), 242–271, DOI: [10.1111/prd.12327](https://doi.org/10.1111/prd.12327).
- 117 P. Scheltens, B. De Strooper, M. Kivipelto, H. Holstege, G. Chételat, C. E. Teunissen, J. Cummings and W. M. van der Flier, Alzheimer's disease, *Lancet*, 2021, **397**, 1577–1590, DOI: [10.1016/S0140-6736\(20\)32205-4](https://doi.org/10.1016/S0140-6736(20)32205-4).
- 118 J.-C. Lambert, A. Ramirez, B. Grenier-Boley and C. Bellenguez, Step by step: towards a better understanding of the genetic architecture of Alzheimer's disease, *Mol. Psychiatry*, 2023, **28**, 2716–2727, DOI: [10.1038/s41380-023-02076-1](https://doi.org/10.1038/s41380-023-02076-1).
- 119 D. T. Wu, Y. W. Cho, M. D. Spalti, M. Bishara and T. T. Nguyen, The link between periodontitis and Alzheimer's disease – emerging clinical evidence, *Dent. Rev.*, 2023, **3**, 100062, DOI: [10.1016/j.dentre.2022.100062](https://doi.org/10.1016/j.dentre.2022.100062).
- 120 M. A. Beydoun, H. A. Beydoun, S. Hossain, Z. W. El-Hajj, J. Weiss and A. B. Zonderman, Clinical and Bacterial Markers of Periodontitis and Their Association with Incident All-Cause and Alzheimer's Disease Dementia in a Large National Survey, *J. Alzheimer's Dis.*, 2020, **75**, 157–172, DOI: [10.3233/JAD-200064](https://doi.org/10.3233/JAD-200064).
- 121 M. H. D. F. Zakaria, S. Sonoda, H. Kato, L. Ma, N. Uehara, Y. Kumoto-Nakamura, M. M. Sharifa, L. Yu, L. Dai, E. Yamauchi-Tomoda, R. Aijima, H. Yamaza, F. Nishimura and T. Yamaza, Erythropoietin receptor signal is crucial for periodontal ligament stem cell-based tissue reconstruction in periodontal disease, *Sci. Rep.*, 2024, **14**, 6719, DOI: [10.1038/s41598-024-57361-y](https://doi.org/10.1038/s41598-024-57361-y).
- 122 A. Sharma, L. Angnes, N. Sattarahmady, M. Negahdary and H. Heli, Electrochemical Immunosensors Developed for Amyloid-Beta and Tau Proteins, Leading Biomarkers of Alzheimer's Disease, *Biosensors (Basel)*, 2023, **13**, 742, DOI: [10.3390/bios13070742](https://doi.org/10.3390/bios13070742).
- 123 C. Peng, R. Pang, J. Li and E. Wang, Current Advances on the Single-Atom Nanozyme and Its Bioapplications, *Adv. Mater.*, 2024, **36**(10), 2211724, DOI: [10.1002/adma.202211724](https://doi.org/10.1002/adma.202211724).
- 124 M. A. Busche and B. T. Hyman, Synergy between amyloid- $\beta$  and tau in Alzheimer's disease, *Nat. Neurosci.*, 2020, **23**, 1183–1193.
- 125 D. R. Thal, U. Rüb, M. Orantes and H. Braak, Phases of A $\beta$ -deposition in the human brain and its relevance for the development of AD, *Neurology*, 2002, **58**, 1791–1800.
- 126 H. Hampel, R. Vassar, B. De Strooper, J. Hardy, M. Willem, N. Singh, J. Zhou, R. Yan, E. Vanmechelen and A. De Vos, The  $\beta$ -secretase BACE1 in Alzheimer's disease, *Biol. Psychiatry*, 2021, **89**, 745–756.
- 127 A. Baranwal, S. Polash, V. Aralappanavar, B. Behera, V. Bansal and R. Shukla, Recent Progress and Prospect of Metal–Organic Framework-Based Nanozymes in Biomedical Application, *Nanomaterials*, 2024, **14**, 244, DOI: [10.3390/nano14030244](https://doi.org/10.3390/nano14030244).
- 128 R. Camedda, C. G. Bonomi, M. G. Di Donna and A. Chiaravalloti, Functional Correlates of Striatal Dopamine Transporter Cerebrospinal Fluid Levels in Alzheimer's Disease: A Preliminary 18F-FDG PET/CT Study, *Int. J. Mol. Sci.*, 2023, **24**, 751, DOI: [10.3390/ijms24010751](https://doi.org/10.3390/ijms24010751).
- 129 G. Chellasamy, S. K. Arumugasamy, M. J. Nam, S. Venkateswarlu, E. Varathan, K. Sekar, K. Manokaran, M.-J. Choi, S. Govindaraju and K. Yun, Experimental and simulation studies of bioinspired Au-enhanced copper single atom catalysts towards real-time expeditious dopamine sensing on human neuronal cell, *Chem. Eng. J.*, 2023, **471**, 144842, DOI: [10.1016/j.cej.2023.144842](https://doi.org/10.1016/j.cej.2023.144842).
- 130 J. Wu, Y. Wu, L. Lu, D. Zhang and X. Wang, Single-atom Au catalyst loaded on CeO<sub>2</sub>: A novel single-atom nanozyme electrochemical H<sub>2</sub>O<sub>2</sub> sensor, *Talanta Open*, 2021, **4**, 100075, DOI: [10.1016/j.talo.2021.100075](https://doi.org/10.1016/j.talo.2021.100075).
- 131 M. Wang, L. Liu, X. Xie, X. Zhou, Z. Lin and X. Su, Single-atom iron containing nanozyme with peroxidase-like activity and copper nanoclusters based ratio fluorescent strategy for acetylcholinesterase activity sensing, *Sens. Actuators, B*, 2020, **313**, 128023, DOI: [10.1016/j.snb.2020.128023](https://doi.org/10.1016/j.snb.2020.128023).
- 132 M. Wang, L. Liu, X. Xie, X. Zhou, Z. Lin and X. Su, Single-atom iron containing nanozyme with peroxidase-like activity and copper nanoclusters based ratio fluorescent strategy for acetylcholinesterase activity sensing, *Sens. Actuators, B*, 2020, **313**, 128023, DOI: [10.1016/j.snb.2020.128023](https://doi.org/10.1016/j.snb.2020.128023).
- 133 Z. Zhao, X. Shi, Z. Shen, Y. Gu, L. He, M. Zhang and N. Lu, Single-atom Fe nanozymes coupling with atomic clusters as superior oxidase mimics for ratiometric fluorescence detection, *Chem. Eng. J.*, 2023, **469**, 143923, DOI: [10.1016/j.cej.2023.143923](https://doi.org/10.1016/j.cej.2023.143923).
- 134 Y. Gu, Z. Cao, M. Zhao, Y. Xu and N. Lu, Single-Atom Fe Nanozyme with Enhanced Oxidase-like Activity for the Colorimetric Detection of Ascorbic Acid and Glutathione, *Biosensors*, 2023, **13**, 487, DOI: [10.3390/bios13040487](https://doi.org/10.3390/bios13040487).
- 135 Y. Wu, L. Jiao, X. Luo, W. Xu, X. Wei, H. Wang, H. Yan, W. Gu, B. Z. Xu, D. Du, Y. Lin and C. Zhu, Oxidase-Like Fe-N-C Single-Atom Nanozymes for the Detection of Acetylcholinesterase Activity, *Small*, 2019, **15**(43), 1903108, DOI: [10.1002/smll.201903108](https://doi.org/10.1002/smll.201903108).
- 136 X. Liu, H. Ding, B. Hu, F. Tian, J. Sun, L. Jin and R. Yang, Large-scale synthesis of high loading Co single-atom catalyst with efficient oxidase-like activity for the colorimetric detection of acid phosphatase, *Appl. Surf. Sci.*, 2022, **605**, 154766, DOI: [10.1016/j.apsusc.2022.154766](https://doi.org/10.1016/j.apsusc.2022.154766).
- 137 Q. Sun, X. Xu, S. Liu, X. Wu, C. Yin, M. Wu, Y. Chen, N. Niu, L. Chen and F. Bai, Mo Single-Atom Nanozyme Anchored to the 2D N-Doped Carbon Film: Catalytic Mechanism, Visual Monitoring of Choline, and Evaluation

- of Intracellular ROS Generation, *ACS Appl. Mater. Interfaces*, 2023, **15**, 36124–36134, DOI: [10.1021/acsami.3c04761](https://doi.org/10.1021/acsami.3c04761).
- 138 Y. Wu, J. Wu, L. Jiao, W. Xu, H. Wang, X. Wei, W. Gu, G. Ren, N. Zhang, Q. Zhang, L. Huang, L. Gu and C. Zhu, Cascade Reaction System Integrating Single-Atom Nanozymes with Abundant Cu Sites for Enhanced Biosensing, *Anal. Chem.*, 2020, **92**, 3373–3379, DOI: [10.1021/acs.analchem.9b05437](https://doi.org/10.1021/acs.analchem.9b05437).
- 139 S. Ding, Z. Lyu, L. Fang, T. Li, W. Zhu, S. Li, X. Li, J. Li, D. Du and Y. Lin, Single-Atomic Site Catalyst with Heme Enzymes-Like Active Sites for Electrochemical Sensing of Hydrogen Peroxide, *Small*, 2021, **17**(25), 2100664, DOI: [10.1002/sml.202100664](https://doi.org/10.1002/sml.202100664).
- 140 M. Wang, L. Liu, X. Xie, X. Zhou, Z. Lin and X. Su, Single-atom iron containing nanozyme with peroxidase-like activity and copper nanoclusters based ratio fluorescent strategy for acetylcholinesterase activity sensing, *Sens. Actuators, B*, 2020, **313**, 128023, DOI: [10.1016/j.snb.2020.128023](https://doi.org/10.1016/j.snb.2020.128023).
- 141 J. Wu, Y. Wu, L. Lu, D. Zhang and X. Wang, Single-atom Au catalyst loaded on CeO<sub>2</sub>: A novel single-atom nanozyme electrochemical H<sub>2</sub>O<sub>2</sub> sensor, *Talanta Open*, 2021, **4**, 100075, DOI: [10.1016/j.talo.2021.100075](https://doi.org/10.1016/j.talo.2021.100075).
- 142 J. Guan, M. Wang, R. Ma, Q. Liu, X. Sun, Y. Xiong and X. Chen, Single-atom Rh nanozyme: An efficient catalyst for highly sensitive colorimetric detection of acetylcholinesterase activity and adrenaline, *Sens. Actuators, B*, 2023, **375**, 132972, DOI: [10.1016/j.snb.2022.132972](https://doi.org/10.1016/j.snb.2022.132972).
- 143 Y. Zhang, H. Chen, R. Li, K. Sterling and W. Song, Amyloid  $\beta$ -based therapy for Alzheimer's disease: challenges, successes and future, *Signal Transduction Targeted Ther.*, 2023, **8**, 248, DOI: [10.1038/s41392-023-01484-7](https://doi.org/10.1038/s41392-023-01484-7).
- 144 S. S. Gupta, V. Mishra, M. D. Mukherjee, P. Saini and K. R. Ranjan, Amino acid derived biopolymers: Recent advances and biomedical applications, *Int. J. Biol. Macromol.*, 2021, **188**, 542–567, DOI: [10.1016/j.ijbiomac.2021.08.036](https://doi.org/10.1016/j.ijbiomac.2021.08.036).
- 145 X. Xiao, X. Hu, Q. Liu, Y. Zhang, G.-J. Zhang and S. Chen, Single-atom nanozymes as promising catalysts for biosensing and biomedical applications, *Inorg. Chem. Front.*, 2023, **10**, 4289–4312.
- 146 B. Dwivedi, P. K. Mishra and V. Mishra, in *Chiral Metal-Organic Frameworks for Asymmetrical Catalysis, Metal-Organic Frameworks (MOFs) as Catalysts*, ed. S. Gulati, Springer Nature Singapore, Singapore, 2022, pp. 493–513, DOI: [10.1007/978-981-16-7959-9\\_19](https://doi.org/10.1007/978-981-16-7959-9_19).
- 147 N. Yadav, D. Mudgal, M. Mishra and V. Mishra, Asparagus officinalis Herb-derived Carbon Quantum Dots: Luminescent Probe for Medical Diagnostics, *Chem. Biod.*, 2024, e202400891.
- 148 N. Yadav, D. Mudgal and V. Mishra, In-situ synthesis of ionic liquid-based-carbon quantum dots as fluorescence probe for hemoglobin detection, *Anal. Chim. Acta*, 2023, **1272**, 341502.
- 149 N. Yadav, D. Mudgal and V. Mishra, Nanobiotic Formulations utilizing Quinoline-based-triazole Functionalized Carbon Quantum Dots via Click Chemistry for Combatting Clinical-Resistant Bacterial Pathogens, *Indian J. Microbiol.*, 2024, 1–15, DOI: [10.1007/S12088-024-01266-x](https://doi.org/10.1007/S12088-024-01266-x).
- 150 N. Yadav, D. Mudgal, A. Mishra, S. Shukla, T. Malik and V. Mishra, Harnessing fluorescent carbon quantum dots from natural resource for advancing sweat latent fingerprint recognition with machine learning algorithms for enhanced human identification, *PLoS One*, 2024, **19**, e0296270.
- 151 M.-H. Chan, B.-G. Chen, W.-T. Huang, T.-Y. Su, M. Hsiao and R.-S. Liu, Tunable single-atom nanozyme catalytic system for biological applications of therapy and diagnosis, *Mater. Today Adv.*, 2023, **17**, 100342, DOI: [10.1016/j.mtadv.2023.100342](https://doi.org/10.1016/j.mtadv.2023.100342).
- 152 X. Zhang, G. Li, G. Chen, D. Wu, X. Zhou and Y. Wu, Single-atom nanozymes: A rising star for biosensing and biomedicine, *Coord. Chem. Rev.*, 2020, **418**, 213376, DOI: [10.1016/j.ccr.2020.213376](https://doi.org/10.1016/j.ccr.2020.213376).
- 153 Q. Zhang, L. Song and K. Zhang, Breakthroughs in nanozyme-inspired application diversity, *Mater. Chem. Front.*, 2023, **7**, 44–64, DOI: [10.1039/D2QM00960A](https://doi.org/10.1039/D2QM00960A).
- 154 Y. Hong, A. Boiti, D. Vallone and N. S. Foulkes, Reactive oxygen species signaling and oxidative stress: transcriptional regulation and evolution, *Antioxidants*, 2024, **13**, 312.
- 155 C. Zhao, C. Xiong, X. Liu, M. Qiao, Z. Li, T. Yuan, J. Wang, Y. Qu, X. Wang, F. Zhou, Q. Xu, S. Wang, M. Chen, W. Wang, Y. Li, T. Yao, Y. Wu and Y. Li, Unraveling the enzyme-like activity of heterogeneous single atom catalyst, *Chem. Commun.*, 2019, **55**, 2285–2288, DOI: [10.1039/C9CC00199A](https://doi.org/10.1039/C9CC00199A).
- 156 L. Jiao, W. Xu, H. Yan, Y. Wu, C. Liu, D. Du, Y. Lin and C. Zhu, Fe–N–C single-atom nanozymes for the intracellular hydrogen peroxide detection, *Anal. Chem.*, 2019, **91**, 11994–11999.
- 157 R. Yan, S. Sun, J. Yang, W. Long, J. Wang, X. Mu, Q. Li, W. Hao, S. Zhang, H. Liu, Y. Gao, L. Ouyang, J. Chen, S. Liu, X.-D. Zhang and D. Ming, Nanozyme-Based Bandage with Single-Atom Catalysis for Brain Trauma, *ACS Nano*, 2019, **13**, 11552–11560, DOI: [10.1021/acs.nano.9b05075](https://doi.org/10.1021/acs.nano.9b05075).
- 158 B. Xu, H. Wang, W. Wang, L. Gao, S. Li, X. Pan, H. Wang, H. Yang, X. Meng, Q. Wu, L. Zheng, S. Chen, X. Shi, K. Fan, X. Yan and H. Liu, A Single-Atom Nanozyme for Wound Disinfection Applications, *Angew. Chem., Int. Ed.*, 2019, **58**, 4911–4916, DOI: [10.1002/anie.201813994](https://doi.org/10.1002/anie.201813994).
- 159 L. Wang, X. Qu, Y. Zhao, Y. Weng, G. I. N. Waterhouse, H. Yan, S. Guan and S. Zhou, Exploiting Single Atom Iron Centers in a Porphyrin-like MOF for Efficient Cancer Phototherapy, *ACS Appl. Mater. Interfaces*, 2019, **11**, 35228–35237, DOI: [10.1021/acsami.9b11238](https://doi.org/10.1021/acsami.9b11238).
- 160 M. Huo, L. Wang, H. Zhang, L. Zhang, Y. Chen and J. Shi, Construction of Single-Iron-Atom Nanocatalysts for Highly Efficient Catalytic Antibiotics, *Small*, 2019, **15**(31), 1901834, DOI: [10.1002/sml.201901834](https://doi.org/10.1002/sml.201901834).
- 161 F. Cao, L. Zhang, Y. You, L. Zheng, J. Ren and X. Qu, An Enzyme-Mimicking Single-Atom Catalyst as an Efficient Multiple Reactive Oxygen and Nitrogen Species Scavenger for Sepsis Management, *Angew. Chem., Int. Ed.*, 2020, **59**, 5108–5115, DOI: [10.1002/anie.201912182](https://doi.org/10.1002/anie.201912182).

- 162 Q. Chen, S. Li, Y. Liu, X. Zhang, Y. Tang, H. Chai and Y. Huang, Size-controllable Fe-N/C single-atom nanozyme with exceptional oxidase-like activity for sensitive detection of alkaline phosphatase, *Sens. Actuators, B*, 2020, **305**, 127511.
- 163 Y. Zeng, E. Almatrafi, W. Xia, B. Song, W. Xiong, M. Cheng, Z. Wang, Y. Liang, G. Zeng and C. Zhou, Nitrogen-doped carbon-based single-atom Fe catalysts: Synthesis, properties, and applications in advanced oxidation processes, *Coord. Chem. Rev.*, 2023, **475**, 214874, DOI: [10.1016/j.ccr.2022.214874](https://doi.org/10.1016/j.ccr.2022.214874).
- 164 P. Xia, C. Wang, Q. He, Z. Ye and I. Sirés, MOF-derived single-atom catalysts: The next frontier in advanced oxidation for water treatment, *Chem. Eng. J.*, 2023, **452**, 139446, DOI: [10.1016/j.cej.2022.139446](https://doi.org/10.1016/j.cej.2022.139446).
- 165 S. Lv, H. Wang, Y. Zhou, D. Tang and S. Bi, Recent advances in heterogeneous single-atom nanomaterials: From engineered metal-support interaction to applications in sensors, *Coord. Chem. Rev.*, 2023, **478**, 214976, DOI: [10.1016/j.ccr.2022.214976](https://doi.org/10.1016/j.ccr.2022.214976).
- 166 A. Iemhoff, M. Vennewald and R. Palkovits, Single-Atom Catalysts on Covalent Triazine Frameworks: at the Crossroad between Homogeneous and Heterogeneous Catalysis, *Angew. Chem., Int. Ed.*, 2023, **62**(7), e202212015, DOI: [10.1002/anie.202212015](https://doi.org/10.1002/anie.202212015).
- 167 J. Fang, Q. Chen, Z. Li, J. Mao and Y. Li, The synthesis of single-atom catalysts for heterogeneous catalysis, *Chem. Commun.*, 2023, **59**, 2854–2868, DOI: [10.1039/D2CC06406E](https://doi.org/10.1039/D2CC06406E).
- 168 R. Chen, S. Chen, L. Wang and D. Wang, Nanoscale Metal Particle Modified Single-Atom Catalyst: Synthesis, Characterization, and Application, *Adv. Mater.*, 2024, **36**(2), 2304713, DOI: [10.1002/adma.202304713](https://doi.org/10.1002/adma.202304713).
- 169 H. Huang, Z. Wang, L. Chen, H. Yu and Y. Chen, Catalytic Biomaterials and Nanomedicines with Exogenous and Endogenous Activations, *Adv. Healthc. Mater.*, 2023, **12**(16), 2201607, DOI: [10.1002/adhm.202201607](https://doi.org/10.1002/adhm.202201607).
- 170 A. Ahmad, S. Tariq, I. Ahmad and N. Arsh, in *Advantages of using MOFs as single-atom catalysts*, *Nanomaterial-Based Metal Organic Frameworks for Single Atom Catalysis*, Elsevier, 2023, pp. 311–329, DOI: [10.1016/B978-0-12-824524-8.00001-3](https://doi.org/10.1016/B978-0-12-824524-8.00001-3).
- 171 Y. Zhu, Y. Liao, J. Zou, J. Cheng, Y. Pan, L. Lin and X. Chen, Engineering Single-Atom Nanozymes for Catalytic Biomedical Applications, *Small*, 2023, **19**(30), 2300750, DOI: [10.1002/smll.202300750](https://doi.org/10.1002/smll.202300750).
- 172 Z. Lyu, J. Zhou, S. Ding, D. Du, J. Wang, Y. Liu and Y. Lin, Recent advances in single-atom nanozymes for colorimetric biosensing, *TrAC, Trends Anal. Chem.*, 2023, **168**, 117280, DOI: [10.1016/j.trac.2023.117280](https://doi.org/10.1016/j.trac.2023.117280).
- 173 V. Kandathil and S. A. Patil, Single-atom nanozymes and environmental catalysis: A perspective, *Adv. Colloid Interface Sci.*, 2021, **294**, 102485, DOI: [10.1016/j.cis.2021.102485](https://doi.org/10.1016/j.cis.2021.102485).
- 174 M. Zhao, N. Zhang, R. Yang, D. Chen and Y. Zhao, Which is Better for Nanomedicines: Nanocatalysts or Single-Atom Catalysts?, *Adv. Healthc. Mater.*, 2021, **10**(8), 2001897, DOI: [10.1002/adhm.202001897](https://doi.org/10.1002/adhm.202001897).
- 175 X. Zhang, G. Li, G. Chen, D. Wu, X. Zhou and Y. Wu, Single-atom nanozymes: A rising star for biosensing and biomedicine, *Coord. Chem. Rev.*, 2020, **418**, 213376, DOI: [10.1016/j.ccr.2020.213376](https://doi.org/10.1016/j.ccr.2020.213376).
- 176 D. Li, F. Zhang, L. Luo, Y. Shang, S. Yang, J. Wang, W. Chen and Z. Liu, A universal strategy for green synthesis of biomass-based transition metal single-atom catalysts by simple hydrothermal and compression treatment, *Chem. Eng. J.*, 2023, **461**, 142104, DOI: [10.1016/j.cej.2023.142104](https://doi.org/10.1016/j.cej.2023.142104).
- 177 J. Liu, Catalysis by Supported Single Metal Atoms, *ACS Catal.*, 2017, **7**, 34–59, DOI: [10.1021/acscatal.6b01534](https://doi.org/10.1021/acscatal.6b01534).
- 178 D. Zhang, D. Kukkar, H. Kaur and K.-H. Kim, Recent advances in the synthesis and applications of single-atom nanozymes in food safety monitoring, *Adv. Colloid Interface Sci.*, 2023, **319**, 102968, DOI: [10.1016/j.cis.2023.102968](https://doi.org/10.1016/j.cis.2023.102968).
- 179 G. Li, H. Liu, T. Hu, F. Pu, J. Ren and X. Qu, Dimensionality Engineering of Single-Atom Nanozyme for Efficient Peroxidase-Mimicking, *J. Am. Chem. Soc.*, 2023, **145**, 16835–16842, DOI: [10.1021/jacs.3c05162](https://doi.org/10.1021/jacs.3c05162).
- 180 S. Ma, W. Han, W. Han, F. Dong and Z. Tang, Recent advances and future perspectives in MOF-derived single-atom catalysts and their application: a review, *J. Mater. Chem. A*, 2023, **11**, 3315–3363, DOI: [10.1039/D2TA08735A](https://doi.org/10.1039/D2TA08735A).
- 181 W. Guo, Z. Wang, X. Wang and Y. Wu, General Design Concept for Single-Atom Catalysts toward Heterogeneous Catalysis, *Adv. Mater.*, 2021, **33**(34), 2004287, DOI: [10.1002/adma.202004287](https://doi.org/10.1002/adma.202004287).
- 182 J. Li, C. Chen, L. Xu, Y. Zhang, W. Wei, E. Zhao, Y. Wu and C. Chen, Challenges and Perspectives of Single-Atom-Based Catalysts for Electrochemical Reactions, *JACS Au*, 2023, **3**, 736–755, DOI: [10.1021/jacsau.3c00001](https://doi.org/10.1021/jacsau.3c00001).
- 183 Y. Yang, Y. Yang, Z. Pei, K. H. Wu, C. Tan, H. Wang, L. Wei, A. Mahmood, C. Yan, J. Dong, S. Zhao and Y. Chen, Recent Progress of Carbon-Supported Single-Atom Catalysts for Energy Conversion and Storage, *Matter*, 2020, **3**, 1442–1476, DOI: [10.1016/j.matt.2020.07.032](https://doi.org/10.1016/j.matt.2020.07.032).
- 184 S. Das, A. Kundu, T. Kula and N. C. Murmu, Recent advancements on designing transition metal-based carbon-supported single atom catalysts for oxygen electrocatalysis: Miles to go for sustainable Zn-air batteries, *Energy Storage Mater.*, 2023, **61**, 102890, DOI: [10.1016/j.ensm.2023.102890](https://doi.org/10.1016/j.ensm.2023.102890).